Open Access

SCHOLARENA

Journal of Material Science and Metallurgy

REVIEW ARTICLE

The Equation of State of Liquid and Solid Materials Part V: Relation with Electrical Resistivity

Jacques Rault*

Laboratory of Solids Physics, CNRS, Paris-Sud University, France

***Corresponding author:** Jacques Rault, Laboratory of Solids Physics, CNRS, Paris-Sud University, France, Tel: 0630976727, E-mail: Jacques.rault@yahoo.fr

Citation: Jacques Rault (2021) The Equation of State of Liquid and Solid Materials Part V: Relation with Electrical Resistivity. J Mate Sci Metall 2: 103

Abstract

Since the pioneer work of Bridgman it is known that the electrical resistance R and the volume V of most crystallizable materials (CM) at low pressure (P<P*) vary similarly with the pressure in great domains of temperature (T > T*0). In these CM V and R vary linearly with T without discontinuity at the Debye temperature. It has been shown that the Modified Van der Waals Equation of State (m-VW EOS), V-V*=(V0-V*)P*/(P+P*) dependent on the characteristic parameters P* and V* and on the initial volume V0(T) at P=0 explains the V-T-P properties of simple elements and compounds (Eur. Phys. J. B 92 (22), 31, 2019). In "normal" CM (dR/dP<0), assuming the R ~ V conjecture, it is shown that the resistivity and volume follows the same R(T,P) and V(T,P) EOS and explains the observed properties : a) The Fan Structure of the Tangents (FST) to the isotherm curves R(P) and V(P) with the convergence points at R*, P* and V*, P*. b) The FST to the isobar curves R(T) and V(T) with the convergence points at R*, T* and V*, T*. c) The superposition principle of the isotherms V(P) and R(P); the thermal pressures (dP/dT)V and (dP/dT)R at constant volume and resistivity are independent on the state (liquid or crystalline) of the element. These thermal pressures are of the same order and same sign as the slope dP/dTtr (or dP/dTm) of the crystalline transition curve (or melting curve) appearing in the T-P domain of measurements. d) The volume and resistivity jumps ΔVm and ΔRm at the melting temperature vary linearly with P and extrapolate to 0 at P*, the ratio of the thermal components of volume and resistivity VmL/ Vms and RmL/ Rms is of the same order. In "abnormal" CM (dR/dP>0) the conjecture V ~ R is not observed but the superposition principle of the curves R(T,P) is still observed in a well-defined T and P domain. In both types of CM the relation (dP/dT)V = (dP/dT)R = dP/dTtr deduced from the Bridgman and Slater conjectures is verified. The resistivity and volume properties of alkali (Na, K, Cs), metals (Hg, Pb, Fe, Sn, Sr), black Phosphorus, Bismuth, metallic glasses and hydrogen studied by Bridgman and others authors are re-analyzed according to this R ~ V conjecture in the framework of the m-VW EOS.

Keywords: Equation of State of Materials, Relation between Volume and Resistivty, Crystalline Transition, Melting Transition

Introduction

About a century ago, Bridgman was the first author who studied in detail the Pressure-Volume-Temperature (PVT) properties of solids and their electrical resistivity ρ (or resistance R). In his reviews [1] [2] and book [3] published later, about 70 years ago, this author classified the metallic elements in two categories: "normal" (dR/dP<0) and "abnormal" (dR/dP>0) materials depending on the pressure dependence of the resistivity (resistance R at low pressure). The author concluded that the resistivity (or resistance) and the specific volume of most solid and liquid metals called "normal" vary very similarly with temperature and pressure. Since that time the PVT Equation Of State (EOS) of materials (insulators, metals, organics, polymers) have been extensively studied, see the book of Poirier [4] and the review of Stacey [5] . Since the pioneer works of Bridgman the resistivity of metals has been also studied in detail by many others authors, one finds in the reviews of Dugdale et al [6] Lacam et al [7] Meaden [8] Hall [9] and Matula [10] references concerning the various metals. In all these studies the temperature dependence of the resistivity ρ (or R the resistance) is given but the properties of the resistivity and specific volume as function of P and T have never been not compared. In the various textbooks [11,12,13] the phonon contribution to the electrical resistivity depends on the temperature ratio T/Θ, Θ Debye temperature ; according to the theoretical model of Debye Grüneisen and Mott two different domains should be observed : $\rho(T) \sim T$ for $T > \Theta$ and $\rho(T) \sim T^5$ for $T < \Theta$. In all the experimental works it is found in fact that the linear dependence ρ(T) is observed in all the metals at high temperature (above and below the melting temperature) down to a temperature T^*_0 much lower than Θ ($T^*_0 / \Theta = 0.15$), see Figure 15 Chap. 7 of ref [12], the physical interpretation of this temperature about 20 to 40 K and the origin of the residual resistance at T=0 in metallic materials is not discussed in this paper. In Figure 1 one gives as examples the relative resistivity or resistance $R(T)/R_0 = \rho(T) / \rho_0 = R(T) / R_0$ of Pb Ni Au Co and Fe above T^*_0 (V and ρ_0: values at 273 K and

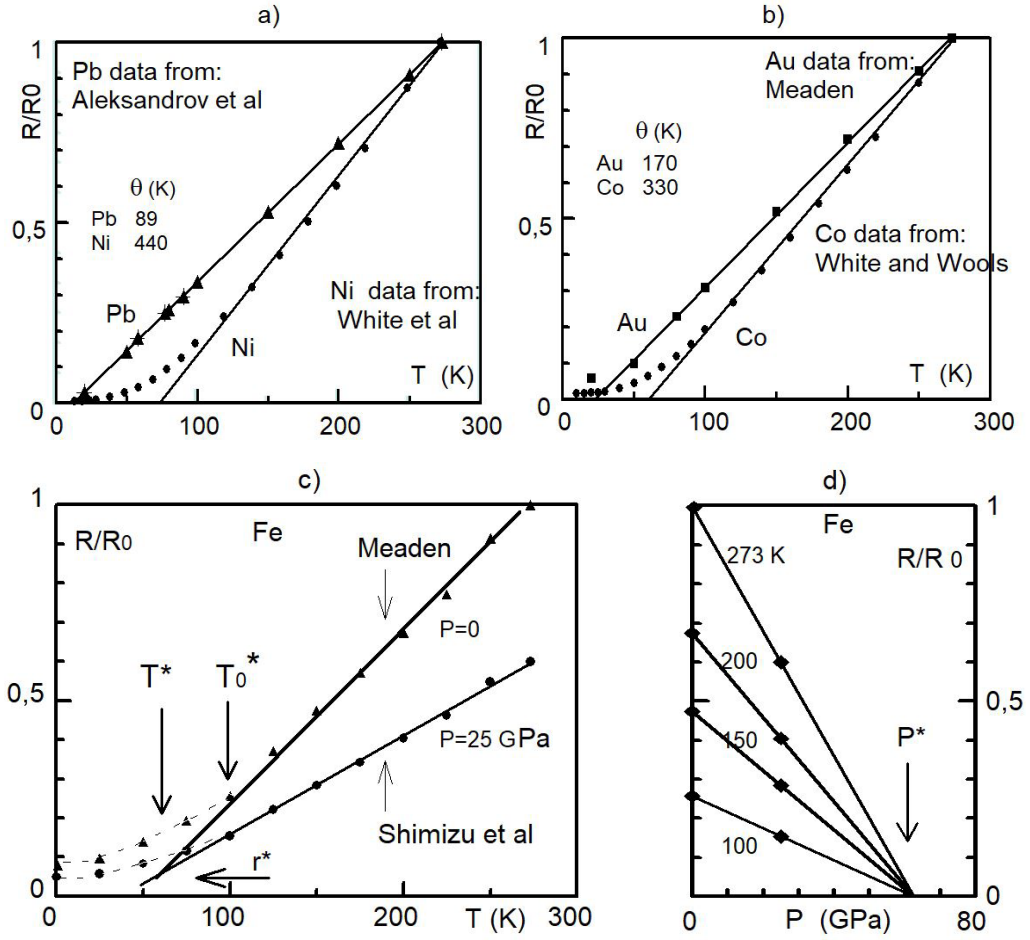

Figure 1: Relative resistivity of various metals between 0 and 273 K at ambient pressure Pb Ni (a) , Au Co (b) and Fe (c,d) at ambient pressure and at 25 GPa. See references in text. R0 is the resistivity at 273 K and P=0. The heavy lines are linear regressions for $T > T0^*$, the Debye temperatures Θ of these metals are indicated

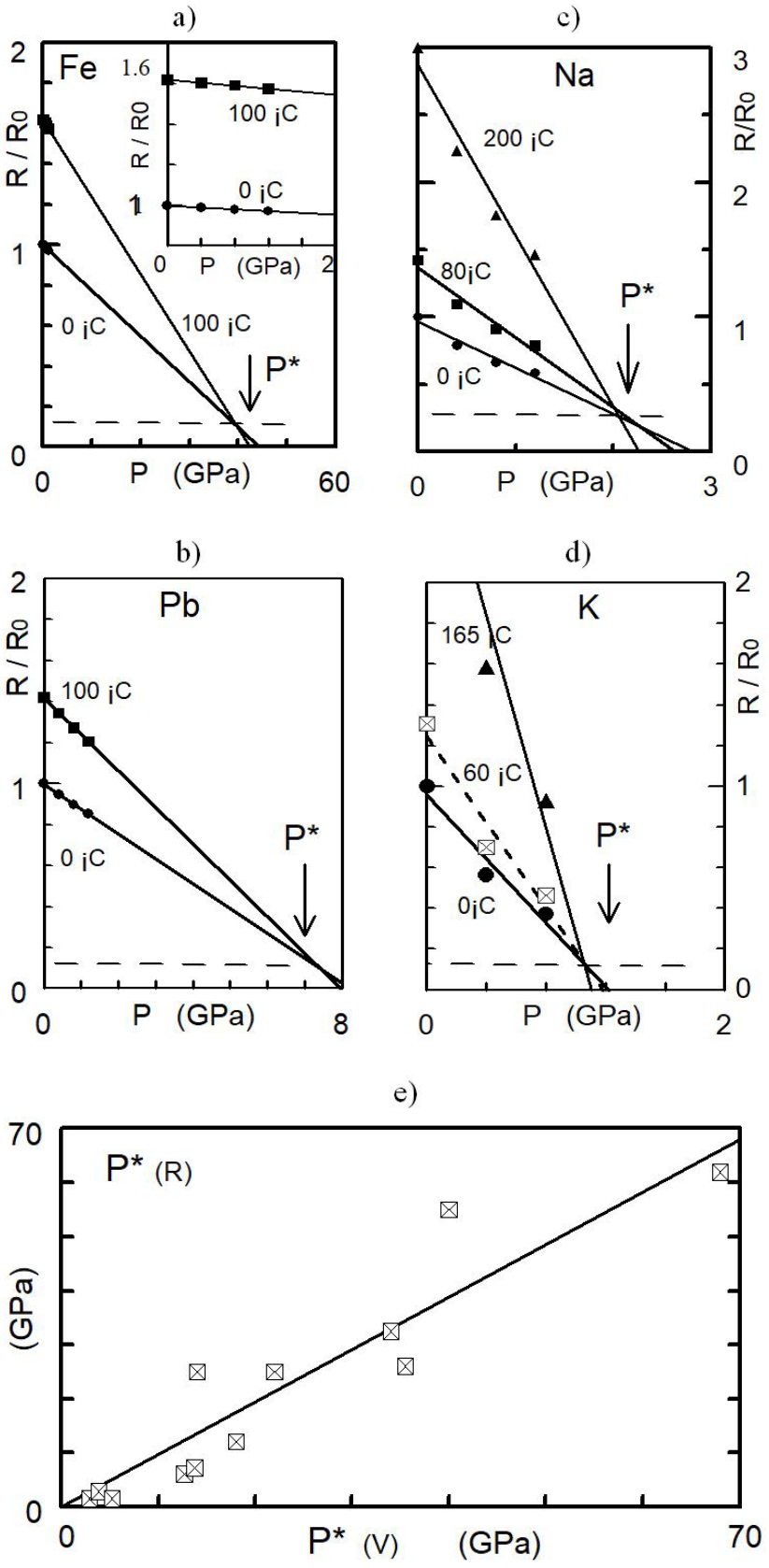

Figure 2: Relative resistivity R/R0 of metals Fe Pb (a,b, solid) and alkali Na K (c, d) solid and liquid (filled triangle) versus pressure at different temperatures, data from Bridgman (Table XIV of ref. [3]). R0 is the resistivity at 0°C and P=0. The linear curves R(P) of the FST-Is at low pressure converge at P*(R) about the characteristic pressure P*(V) deduced from the mVW-EOS relation. e) Relation between the two characteristic pressure P*(R) and P*(V) deduced from the FST-Is and from the m-VW EOS, see Table 2

P=0), the data coming from different authors can be found in the reviews of Meaden and Hall. These authors found also the same similar linear relations in Al Cu and Mo above and below the Debye temperature. In Figure 2 one gives the pressure variations of the relative resistance R(P) / R_0 of Na K Pb and Fe; data are found in Table XIV of the Bridgman book [3], same linear variation R(P) for any constant temperature are observed in all metals (solid or melt). Here again one notes that in most conductor materials (having the "normal" behavior) R and V vary linearly with T at constant P without discontinuity at and vary linearly with P at constant T, at low pressure. These very similar variations of V(T,P) and R(T,P), in the same T and P domains, first observed by Bridgman in "normal" metals, suggest that these two parameters verify the same equation of state.

The aim of this paper is to show that the electrical resistivity of most crystalline and molten pure materials (called "normal" by Bridgman) verifies the modified Van Der Waals equation of state (m-VW EOS) (see ref. [14,15,16,17] if one assumes that V / V_0 and R / R_0 present similar variations with T and P (V_0 and R_0 being reference values (at T=0°C and P=0 for example). Data above T^*_0 of various simple elements (metals and alkali) and alloys in liquid glassy and crystalline states, are re-analyzed. This V~R conjecture is verified at low pressure, whatever is the state (solid or liquid) of the Crystallizable Material (CM) and Glassy Material (GM), whatever is the form of the sample (poly-crystalline or mono-crystal). This conjecture does not apply to "abnormal" elements but the superposition principle is still observed; examples of Phosphorus and Bismuth are given.

The m-VW EOS and the V~R conjecture

The modified Van der Waals EOS and its resistance equivalent write:

$$V - V^* = (V_0 - V^*)\frac{P^*}{(P + P^*)} \quad ; \qquad \text{(m-VW EOS)} \qquad (1a)$$

$$R - R^* = (R_0 - R^*)\frac{P^*}{(P + P^*)} \quad ; \qquad \text{(V~R conjecture)} \qquad (1b)$$

$$X - X^* \approx (X_0 - X^*)(1 - \frac{P}{P^*}) \quad ; \; X = V \; or \; R \; ; \; P < P^* \qquad (1c)$$

At low pressure the reference values V_0 and R_0 at P=0 vary linearly with T in the liquid and solid states (above T^*_0 ~ 20 K) One defines the temperature coefficients of the relative volume and resistivity at constant P: $\alpha(V) = (1/V_{ref})(dV/dT)$ and $\alpha(R) = (1/R_{ref})(dR/dT)$. In the works of Bridgman V_{ref} and R_{ref} are the reference values at 0°C and P=0. In Table 1a these coefficients of alkali and transition metals are compared, α(R) values are deduced from Table XIV of ref. [3] and the α(V) values (thermal expansion) can be found in ref. [12]. The ratio α(R) / α(V) independent on T is about 20 in alkali and 50 to 180 in transition metals. The similar linear variations of V and R with T above and below the melting temperature suggest that this ratio is constant. The relation:

$$[\alpha(R) / \alpha(V)]_{sol} = [\alpha(R) / \alpha(V)]_{liq} \qquad (1d)$$

will be verified for Na. Relation 1b is called the V~R conjecture. The m-VW EOS depending on two parameters, P* and V*, fits with a great accuracy the P-V-T data of polymers and organic compounds in the molten and glassy states [14]. The fit parameters are the same for the three different states (solid amorphous and liquid) and the physical interpretation has been given. The initial values V_0 and R_0 at P=0, are higher than the plateau values V* and R* (P—> ∞) and the relative variations of volume and resistivity with P and T are very similar (rel.1c). The relation between this m-VW EOS determining the thermodynamic properties and the Vogel-Fulcher -Tamann (VFT) relation which rules the rheology of the liquid state have been given in reference [15] and [18]. The relation between the mVW-EOS and the kinetic properties of solid polymers (plastic flow, yield, compensation law) have been discussed in reference [16]. In the following one will compare the R(T,P) and V(T,P) properties of solid and molten metals deduced from rel.1. The V(T, P) properties of CM, solid and liquid (metals and minerals) have been analyzed in reference [17] and are recalled here.

	Na	K	Cs	Fe	Ni	Pb	Ag	Cu	Au	Al	Pd
α(R) (10^{-3} K^{-1})	5	5.4	4.8	6.2	6.3	4.2	4	4,3	3.9	4.6	3.1
α(V) (10^{-6} K^{-1})	210	249	291	35	37.5	86	38	67	41.7	47.2	34
α(R) / α(V)	24	21.6	16	177	168	49	105	64	94	99.5	91
P* (GPa)*	2.9	2.5	1.3	68		18	38	40	50	35	

Table 1a: Thermal expansion and resistivity coefficients, α(V) and α(R), of alkali and transition metals in the solid state near room temperature at P=0. Data at room temperature from Kittel (α_V) and from Bridgman (α_R). P* characteristic pressure deduced from the m-VW EOS

a) T variations of R and V: It known that at high temperature above Tm V and R vary linearly with T at constant pressure. In the solid and liquid states Kaptay, table 3 of ref. [19], have shown that VS and VL of metals verify relation 2a. From the works of Matula one will shown that the resistivities of Au follow a similar relation 2b:

$$V_S = V_{S0} + m_{SV}\, T^n \; ; \quad V_L = V_{L0} + m_{LV}\, T \; ; V_{S0} = V_{L0} = V^* \qquad (2a) \quad (2a)$$

$$R_S = R_{S0} + m_{SR}\, T^n \; ; \qquad R_L = R_{R0} + m_{LR}\, T \; ; R_{R0} = R_{L0} = R^* \qquad (2b) \quad (2b)$$

m_{XY} are constants. For most solid metals the exponent n deduced from the volume $V_S(T)$ at ambient pressure is between 1.3 and 1.5 In solid gold one will verify the same scaling laws V ~ R ~ T^n . The important point to note is that the extrapolated volumes V_{S0} and V_{L0} (and resistivity R_{S0} and R_{L0}) are of the same order. In the following it is shown that the extrapolated volumes of gold are pressure independent and equal to the characteristic volume V* of the EOS (rel.1)

	Ag	Al	Au	Cu	Ir	Ni	Pb	Pd	Pt	Rh
Tm (K)	1235	933.5	1337	1358	2719	1728	600.6	1828	2042	
V_{S0}	10.14	9.87	10.11	7.04	8.48	6.54	17.87	8.8	9.04	8.25
V_{L0}	10.14	9.76	10.15	6.97	8.49	6.71	17.93	8.74	9.09	8.17
v_L/v_S	1.9	1.8	1.72	1.74	2	1.8	1.6	1.7	1.74	2
r_L/r_S	1.9	1.64	2.28	2.07		(2.34)	2.07	1.74	2.4	1.9

Table 1b: Molar volume of liquid and crystalline (fcc) metals deduced from the scaling laws given by Katpay; Vs ~ T^n below Tm and VL ~ T above Tm. v_L/v_S is the ratio of the thermal components of the volumes (liquid and solid) at Tm, data from table 3 ref. (19) rL / rS , data from Mott ref. (11) and Arblaster [20].

FST-Ib: Fan Structure of the Tangent to the Isobars V(T) and R(T)

The FST to the isobars V(T) of polymers and organic materials, in the glassy crystalline and molten states have been discussed in references [14] and [15]. Whatever is the state, solid or liquid, the volume vary linearly with T in a great domain of temperature. In the molten state the FST-Ib of linear polymers and glycerol converge to a point T_{CP} and V_{CP}, in these compounds the characteristic temperature T_{CP} is of the order of the Vogel temperature (where the viscosity and characteristic time of the cooperative motions diverge, see ref. [15]. In crystalline minerals the FST is also observed but the characteristic temperature T_{CP} of the convergent point is negative and up to now has not obviously physical interpretation; examples given in ref. [17]: NaCl (- 4000 K) MgO (-4000 K) and Li (- 1300 K). Hereafter one will compare the isobars V(T) and R(T) of Na, Hg, Pb, Fe, black P.

FST-Is: Fan Structure of the Tangent to the Isotherms V(P) and R(P)

As predicted by rel.1a, in any material the tangents to the isotherms V(P) present a FST; the tangents at P=0 converge to the point P* V*; the P* and V* values so obtained :

$$v^* = \frac{V^*}{V_0} = \frac{B_0' - 1}{B_0' + 1} \; ; \; P^* = \frac{B_0}{\gamma^*} \; ; \; \gamma^* = \frac{1}{2}(B_0' + 1) \qquad (3)$$

(B and B' bulk modulus and its P-derivative) are in total agreement with the values obtained directly by the fit of the experimental data with the m-VW EOS. γ* is the Slater anharmonicity parameter [17,21]. The FST-Is method is the most accurate method for determining these two parameters V* and P* when at least two experimental isotherms V(P) curves are known, even in a small range of pressure, example given hereafter: Fe. Examples of FST to the V(P) isotherms of polymers and CM are given in references [14] and [17] . Same linear variations R(P) are deduced from rel.1b at low pressure, P<P* , at higher pressure the plateau values $v^*=V^*/V_0$ and $r^*=R^*/R_0$ are generally observed. The FST to the R(P) isotherms of crystalline metals are deduced from Table XIV of the Bridgman book, four examples of fan structures (FST-Is) are given in Figure 1d and 2. The characteristic parameters R* and P* are given in the figures. It is important to note that for K and Na this convergent point (R*, P*) does not depend on the state, crystalline or molten, of the element. The P*(R) values deduced from the convergence point of the FST to the R(P) curves are given in Table 2a and compared to the P*(V) values deduced from the m-VW EOS (rel.1a and rel.2). For Hg and alkali metals (Na, K,) the values in bracket are deduced from the m-VW EOS fit, see Table 2 of ref. [17]. For metals the P*(V) values are deduced from rel.2, the B_0 and B'_0 values (at P=0 and at ambient temperature) are given in the reviews of [22,23,24] .

Transition metals have P* pressures one to two orders of magnitude higher than alkali metals. In glass and crystallized materials the relation between the bulk modulus bond energy and characteristic pressure P*(V) has been given, see ref. [14] and [17]. From table 2a one concludes that the pressures P*(V) and P*(R) deduced from the volume V(T,P) and resistivity R(T,P) curves are of the same order. In Figure 2c one shows that the characteristic pressure deduced from the resistivity measurements of Bridgman can be put on the linear form $P^*_{(R)} = 1.06\ P^*_{(V)}$ with a correlation factor Rc=0.934. The accuracy of the resistivity is not given by this author. In ref. [17] the estimated accuracy on $P^*_{(V)}$ is about 15% and depends on the type of EOS used by the different authors (polynome, Murnhagam, Birch EOS) for calculating the bulk modulus and its pressure derivative.

In Table 2b one gives the characteristic parameters $v^*=V/V_0$ and $r^*=R/R_0$ (reference values V_0 and R_0 at ambient condition) deduced from the FST–Is and from the m-VW EOS (rel.2), data and references are given in ref. [17], [23]. As noted by various authors the B' value of these elements is between 3 and 5 then from rel. 3 v* is of the order of 0.6 One verifies that the two evaluation methods give similar v* values. It will be shown that the relative resistivity r* of the "normal" elements analyzed hereafter is of the order of v*/10.

	Na	K	Hg	In	Pb	Sn	Mg	Al	Ag	Au	Cu	Fe
T_1 °C	0	0	50	30	0	0	0	0	0	0	0	0
T_2 °C	80	30	100	75	100	95	100	100	100	100	100	100
$P^*_{(R)}$	1.4	2.8	1.4	6.5	7.2	12	25	26	25	33.4	55	60
$P^*_{(V)}$	(2.9)	(3.8)	(5.2)	12.7	13.7	18	14	35.5	22	34	40	68

Table 2a: Comparison of the characteristic pressures P* (GPa) of various metals. P*(R) is deduced from the FST-Is of the resistivity R(P) curves at P=0 and 4 kbar at T_1 and T_2, data from Bridgman, Table XIV of ref. [3]. P*(V) is deduced from the m-VW EOS, rel.1a and from rel.3 in brackets

	Na	K	Fe	Pb	Sn// ⊥	Zn // ⊥	Hg	H_2
v* FST	0.6	0.32	0.45	0.5			0.8	0.6
v* rel.2	0.65	0.62	0.77	0.75	0.74	0.65		0.75
r*	0.03	0.05	0.05	0.05	0.1 0	0.5 0	0.4	0.07-0

Table 2b: Relative resistivity $r^*= R^*/R_0$ and volume $v^*= V^*/V_0$ of elements deduced from the FST-Is and from the EOS (rel.1), V_0 and R_0 values at ambient temperature and pressure. For Sn and Zn monocrystals the r* values in parallel and perpendicular direction to the c axis are given. For hydrogen V_0 and R_0 are the volume at 90 K at 300 K (v*) and at 20 K (r*). See text

In conclusion from the FST to the resistivity isotherms R(P) at low pressure (P<P*) and then by extrapolation up to P* one will verify the V~R conjecture (rel.1b) suggested by Bridgman. As reported by various authors, see ref. [7], at high pressure this conjecture is no longer observed; the metallic elements become "abnormal", V and R vary inversely (P>>P*: dV/dP<0 and dR/dP>0).

The T-P superposition principle, the α/κ rule

Any isotherm V(P) of a material at temperature at T+ΔT can be superposed with the isotherm at T by a translation ΔP along the P axis. We have shown that this property, the T-P superposition principle, is verified in amorphous materials [14] and in various crystalline compounds [17]. Sanchez et al [25] were the first authors to point out that the "compression response of polymers and organic liquids satisfies a strong temperature-pressure superposition principle". This translation ΔP deduced from rel.1 is independent on P at low pressure:

$$\Delta P = (P^*+P)\frac{V_0(T)-V_0(T+\Delta T)}{V-V^*} \approx P^*\frac{\Delta V_0}{V_0-V^*};\ P<P^* \qquad (4a)$$

the ratio ΔP/ΔT at constant V can be considered T independent as first approximation; the thermal expansion coefficient α is T independent and $V^* < V$. The mVW-EOS and the R ~ V conjecture, rel.1, lead to the thermal pressures $(dP/dT)_V$ and $(dP/dT)_R$ at constant V and constant R:

$$\left(dP/dT\right)_V = \frac{V_0^{'}}{V_0-V^*}\left(P^*+P\right)\ ;\ \left(dP/dT\right)_R = \frac{R_0^{'}}{R_0-R^*}\left(P^*+P\right) \qquad (4b)$$

$$\left(dP/dT\right)_V = \alpha_{(V)}/\kappa_{(V)}\ ;\ \left(dP/dT\right)_R = \alpha_{(R)}/\kappa_{(R)} \qquad (4c)$$

The index (V) and (R) refer to the curves V(T,P) and R(T,P). Rel.4c is deduced from the thermodynamic relation $(dP/dT)_V = -(dV/dT)_P/(dV/dP)_T = \alpha/\kappa$ which gives the ratio between the thermal expansion and compressibility coefficients. From the V ~ R conjecture, rel.1b, one concludes that the same relation applies for $(dP/dT)_R$. α(X) and κ(X) (measured at constant P and T) are the temperature and pressure derivations of the relative volume V/V_{ref} and resistivity R/R_{ref} (V_{ref} and R_{ref} : values at a reference temperature). In references [14] and [17] it has been shown that the thermal pressure deduced from the V(P,T) curves:

$$\alpha B = (\alpha/\kappa)_a = (\alpha/\kappa)_b \qquad (4d)$$

is constant in the different phases a and b of a same material, at melting and at a crystal-crystal transition. This relation between bulk modulus B=1/κ and thermal expansion coefficient α was suggested by Slater [21], noting that the change of entropy dS with volume dV in going from one phase to another is of the same order as the change of volume dV of a single phase. The relation between the thermal pressure and the slope of the transition temperature curve $T_{tr}(P)$ (or $T_m(P)$) is:

$$\alpha B = \left[\frac{dS}{dV}\right]_T = \left[\frac{dP}{dT}\right]_V = k_{tr}\frac{dP}{dT_{tr}}\ ;\ (\alpha B)_{liq} = (\alpha B)_{sol} \qquad (4e)$$

k_{tr} (or k_{Im}) is a constant. In halides (NaCl, AgBr…) k_{Im} ~ 1 and in alkali and metals k_{Im} ~ 2-8 (see Table XVI-2 of ref. [21]. This relation (called the Slatter conjecture) indicates that the sign of dP/dT at constant volume is positive for most materials and negative for material which present a transition temperature decreasing with the pressure. Then the R~V conjecture and the superposition principle leads to the relation between the thermal pressures at constant V and R:

$$\left[\frac{dP}{dT}\right]_V = \left[\frac{dP}{dT}\right]_R \approx \frac{dP}{dT_{tr}} \;\; ; \;\; \left[or \approx \frac{dP}{dT_m}\right] \quad \text{(Slatter conjecture)} \qquad (4f)$$

Hereafter one will show that relations 4 are verified. Examples given hereafter: "normal" elements Na K Hg and "abnormal" elements P Bi Sr.

Volume and resistivity jumps at the melting and crystalline transitions Tm and Ttr

In Table 2 and 3 of ref. [17] we have shown that the characteristic pressures P_{Tm}=Tm0(dP/dTm) and P_{Lm}=(ΔHm/ΔVm) of the alkali and metals are of the same order as the characteristic pressure P* deduced from the m-VW EOS. Same pressures P_{Tr} are defined for any crystalline transition at Ttr. The temperatures of melting (or crystalline transition) of elements vary linearly with P at low pressure (P<P*) then from the experimental linear relation Tm(P) (or Ttr(P) and from the Clapeyron relation,

$$T_m = T_{m0} + \frac{dT_m}{dP} P \; ; \; P_{Tm} = T_{m0} \frac{dP}{dT_m} ; P_{Lm} = \frac{\Delta H_m}{\Delta V_m} ; P_{Tm} = P_{Lm} = P^* \qquad (5a)$$

ΔHm is the melting enthalpy. Same relation is obtained for any crystalline transition at Ttr. One concludes that Tm (or Ttr) extrapolates to 0 K at the pressure P_{Tm}= - P*. This will be verified for the α → β transition of crystalline Hg. The melt and crystalline states of a CM verify the same m-VW EOS, rel.1a, same P* and V* values but different initial volumes Vom and Vos. The volume jump ΔVm at Tm is:

$$\Delta V_m = \Delta V_{oms} \left(\frac{P^*}{P + P^*} \right) \approx \Delta V_{oms} (1 - P / P^*) \; ; \; P < P^* \qquad (5b)$$

ΔVoms = Vom – Vos is the volume jump at Tm(P =0), similar relation is obviously obtained for CM presenting a volume jump ΔVtr at a crystalline transition at Ttr. Grilly et al and Swenson have measured the P dependence of the volume and its jump ΔV at the melting transition of crystalline N_2 [26] and of the α–β transition of Hg [27], their data verify the m-VW EOS (rel.1a and 5b). At low pressure (P<P*) the volume jump ΔVm(P), or ΔVtr(P), extrapolates to zero at P* in total agreement with the P* value deduced from the m-VW EOS. For "normal" elements from the R ~ V conjecture one deduces the linear variation of the resistivity jump ΔRm(P) at melting:

$$\Delta Rm = \Delta R_{0m} \left(\frac{P^*}{P + P^*} \right) \approx \Delta R_{0m} (1 - P / P^*) \; ; \; P < P^* \qquad (5c)$$

Bridgman [2] reported such variations of the jumps ΔVm(P) and ΔRm(P) for different materials. Hereafter one shows that at melting the volume and resistance jumps follow relations 5 and extrapolate to zero for the same characteristic pressure P*, equal to the P* value deduced from the EOS rel.1. Examples given hereafter: Na K and Hg.

Bridgman [1-3] concluded that at the melting transition ΔVm and ΔRm vary in the same direction; positive if the metal expands (most materials) and negative if the metal contract (Ba, Bi, etc) on melting. The expansion and contraction are related to the slope of the melting curve Tm(P) given by the Clapeyron relation dTm/dP = Tm0 ΔVm/ΔHm materials near the glass and melting transition depend also on the sign of the volume jump at the transition.

The Compensation Law

This empirical law is often called the Keyes or Nachtrieb relation [28,29]. The relation between volume and enthalpy activations, ΔVa ΔHa, of the kinetic processes in glass and crystalline materials (auto-diffusion, aging, plastic deformation) near the melting transition or the glassy temperature verify this law, see ref. [15,6,17] and [30,31]. The compensation relation of CM writes:

$$\Delta H_a / \Delta V_a = \Delta H_m / \Delta V_m \quad , \quad P_a = P_{Tm} = P^* \tag{5d}$$

The characteristic pressures $P_a=\Delta H_a/\Delta V_a$ and $P_{Tm}=\Delta Hm/\Delta Vm$ are equal to the characteristic pressure P* deduced from the EOS, rel.1a. In CM it has been verified that the auto-diffusion process has positive or negative volume activations in metals which expand or contract on melting, see ref. [29].

In alkali and transition metals it has been shown [17] that all the characteristic pressures, P_B, P_G, $P_{\sigma y}$, P_{Tm}, deduced from the linear variations of the bulk and shear modulus (B and G) the yield stress (σy) and from the melting temperature (Tm) are of the order of P*:

$$P_{\sigma y} \approx P_B \approx P_G \approx P^* \quad ; \quad P_{Tm} \approx P^* \tag{5e}$$

One concludes that the compensation relation and the above universal relation between the various characteristic pressures have the same origin.

Hereafter one will re-analyze the T and P variations of resistivity of Bismuth and black phosphorus, which are "abnormal" (dR/dP<0) according to the Bridgman classification and which present a melting curve Tm(P) with a negative slope dTm/dP < 0.

Ageing of metallic glass

Metallic glasses are obtained by melt spinning generally at room temperature and then by annealing at a temperature below the glass temperature Tg. Phase separation and crystallization can occur during the process. In atactic polymers (and organic compounds) these last effects do not occur or are much slower. For these reasons the aging properties of these last materials have been studied in great detail [30]. During annealing below Tg (aging) the change of volume and enthalpy (ΔV_{ag}, ΔH_{ag}) and modulus, compliance, yield stress, etc.. vary linearly with the logarithm of the aging time t :

$$\Delta V_{ag} = k_V \log t / \tau_i \; ; \; k_V = C_2 \Delta\alpha / C_1$$
$$\Delta H_{ag} = k_H \log t / \tau_i \; ; \; k_H = C_2 \Delta C_P / C_1 \tag{6a}$$

between the incubation time τ_i and final time τ_f, relaxation times of the liquid having the initial volume V0 and final volume V of solid at the annealing temperature. Δα and ΔCp are the thermal expansion and calorific capacity jumps at the transition. This aging law is explained in the framework of the Vogel-Fulcher-Tamann (VFT) law [18,30]. C_1 and C_2 are the constants of the Williams Landel Ferry (WLF) relation giving the relaxation time τ (or viscosity) of the liquid above Tg; $\log \tau / \tau_g = - C_1(T-T_g) / (T-T_g+C_2)$. It has been shown that the pressure Pag = $\Delta H_{ag}/\Delta V_{ag}$, deduced from the changes of enthalpy and volume during aging, is the characteristic pressure P* deduced from the m-VW EOS [16]. The compliance J permittivity ε yield stress σ_y vary also in a similar manner, then again one postulates that the change of volume and resistivity with the aging time in "non supraconductors" materials vary with the aging time as:

$$\Delta V_{ag} = k_V \log t \; ; \; \Delta R_{ag} = k_R \log t \; ; \tag{6b}$$

Hereafter one will show that the time derivative of the relative volume and resistivity at constant P are of the same order:

$$\frac{d\Delta V / V_0}{d \ln t} = \frac{d\Delta R / R_0}{d \ln t} \tag{6c}$$

Example given hereafter: an Iron based alloy: $Fe_{40}\, Ni_{40}\, B_{20}$

Data Analysis of the Metallic Materials

In the domain of low pressure, P<1.2 GPa, most of metallic elements are "normal" (dR/dP<0), but at higher pressures, P>>2 GPa, these CM are "abnormal" (dR/dP>0). This complex behavior first observed by Bridgman has been reviewed then by Dugdal et al [6] and Lacam et al [7]. This behavior would be due to electronic rearrangements. Hereafter one re-analyzes in the domain of low pressure 8 "normal" metallic elements: 2 alkali, 5 metals, an alloy and two"abnormal" metals. Most of these materials are in the polycrystalline forms, only 4 elements are in the single crystal form (Sn, Zn, Bi, Sr).

Sodium

Makarenko et al [32]have studied in detail the T-P variations of the volume of solid and liquid Na at 7 temperatures up to 1.2 GPa. In Figure 3a one reports the isotherms V(P) of these authors at three temperatures, the data come from Table 1 of their paper. At 493.15K and 433.15 K Na is liquid and at 373.15 K solid. In Figure 3b the relative resistivity measured by Bridgman at 4 temperatures is given, R(P) data are deduced from Figure 68 of ref. [3]. In both Figure 4 the plain lines are the fit with the EOS, rel.1, the P* values are indicated. In Figures 4a,b one compares the linear variations of the volume and relative resistance with T at P=0 of solid and liquid Na. In Figure 4c the relative resistivity at various pressures is reported, data come from Table XIV of the Bridgman book. One verifies that the resistivity curve of solid Na follow the same linear variation with T above and below

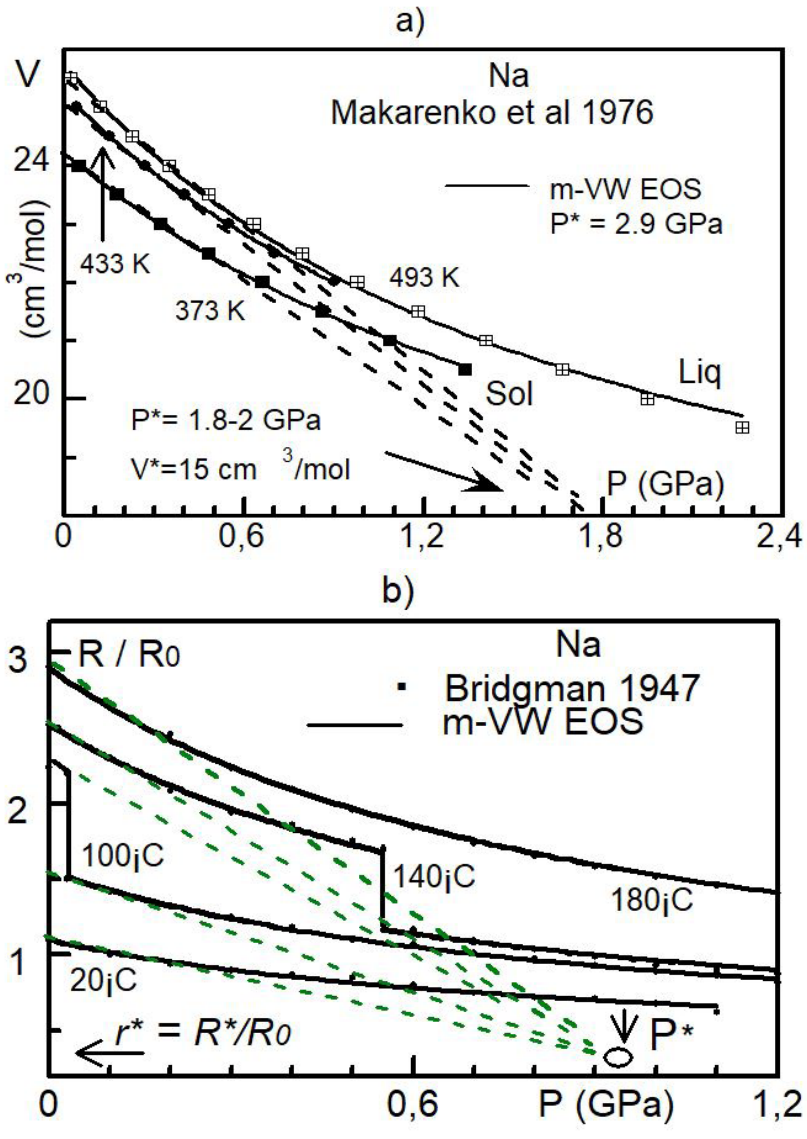

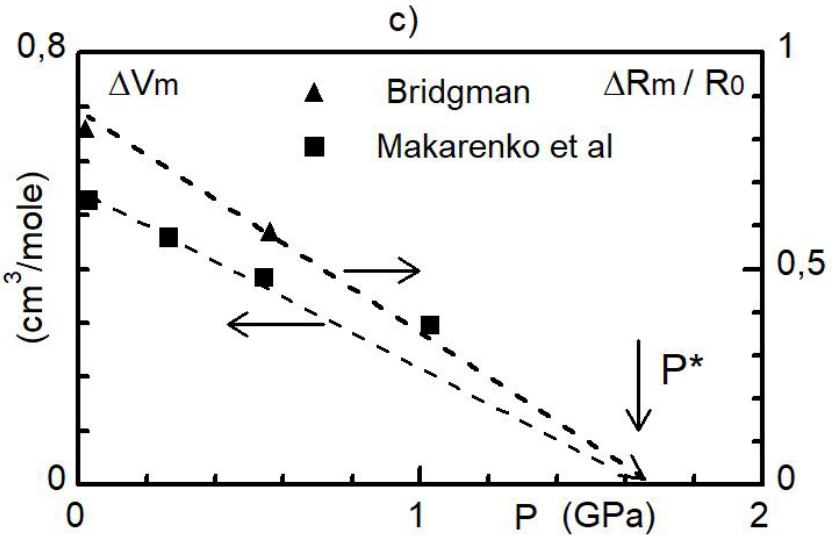

Figure 3: a,b) Volume and relative resistivity of Na (solid and liquid) as function of T and P. Data from Makarenko et al [32] and Bridgman [3]. Heavy lines are the m-VW EOS Fit. FST-Is; dashed lines are the tangents to the V(P) and R(P) isotherms at P=0

c) Volume and resistance jumps at the melting as function of pressure, data deduced from ref. [3] and [32]at low pressure P<P*. Dashed lines, linear regression for P<1 GPa. The characteristic pressure P* deduced from the mVW EOS fit, from the FST to the V(P) and R(P) curves of solid and liquid Na, from the jumps ΔVm and ΔRm are of the same order, see text

the Debye temperature (θ = 63 °C). Also it is important to remark that the linear curves $V_s(T)$ and $V_l(T)$ of the solid and liquid states converge at T*(V) =250 K (Figure 4a). Similarly the curves $R_s(T)$ and $R_l(T)$ converge at T*(R) = 200 K (Figure b). From the convergent point of the Fan Structure of the of isobars R(T) (Figure c) a similar characteristic temperature is found, T*~ 170 K. These properties, similar linear variations V(T) and R(T) and similar extrapolated temperatures T*(V) and T*(R) of solid and liquid Na are clear indications that the conjecture V ~ R at P=0 is verified.

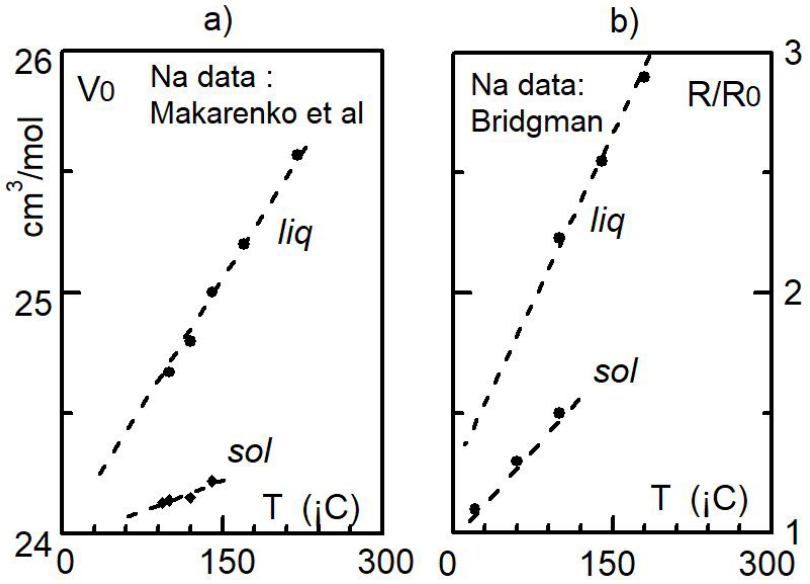

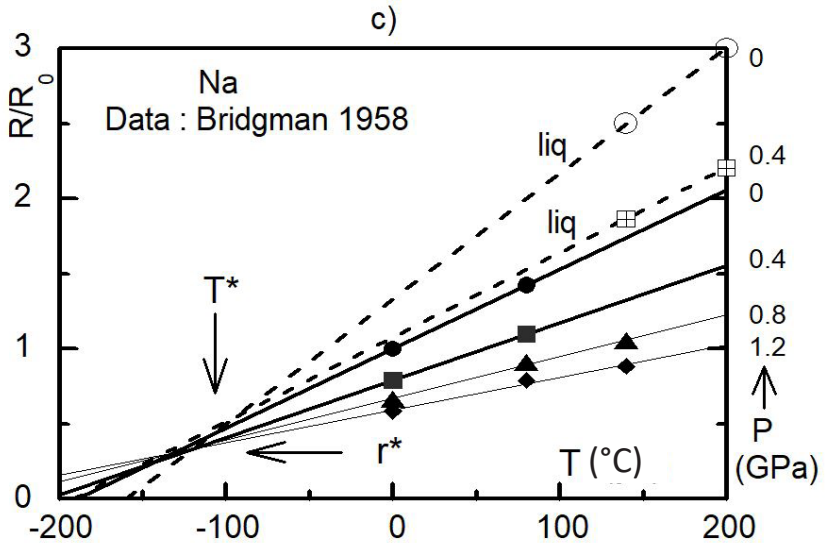

Figure 4: a) and b) relative volume and resistivity of Sodium at P=0 versus T (°C) temperature, V0 and R0 values at 0°C and P=0. Data from Makarenko et al [32] and Bridgman). c) Relative resitivity of solid and liquid Na versus temperature at 4 pressures, plain (solid Na) and dashed (liquid Na) lines are linear regressions). Data from table XIV of ref. [3]

FST-Is

The tangents to the isotherm curves V(P) and R(P) at P=0 present the fan structure, in both cases the convergent point is the same for the solid and liquid state. The characteristic pressure P*(V) and P*(R) at the convergent points of the FST-Is are P*(V) =2.1 ± 0.2 GPa and P*(R) =1 GPa. These values are not far from the values determined directly from the fit of the P-V-T data with the m-VW EOS: P* = 2.9 GPa (see ref. [17]).

In conclusion from the FST to the V(P) and R(P) isotherms of the solid and liquid states one deduces very similar values of the characteristic pressure P*, 2 and 1 GPa, not far from the value, 2.9 GPa, determined directly from the m-VW EOS fit. The characteristic parameters V_0/V^* and R_0/R^* are also somewhat different, respectively 1.6 and 2.8.

Superposition principle and Thermal pressure

One verifies that the isotherms V(P) and R(P) of Makarenko et al and Bridgman can be superposed by simple translation ΔP, the thermal pressures of the solid state are : $(dP/dT)_V = 6.5\ MPaK^{-1}$, $(dP/dT)_R = 4.3\ MPaK^{-1}$. These values are of the same order as the slope dP/dTm = 12 $MPaK^{-1}$ of the melting curve P(Tm), the Slater conjecture is verified with k_{tr} = 1.8 to 2.8 . From the work of Anderson et al [33]we concluded in reference [17] that between 150 and 450 K the superposition principle was also observed, the thermal pressure at constant V has the same value in the solid and liquid state, but its value $(dP/dT)_V = 1.3\ MPaK^{-1}$ is different from the Makarenko et al value (factor 5).

c ΔV_m *and* ΔR_m *jumps.* In Figure 3c it is shown that the volume and relative resistance jumps at the melting can be approximated below P* by linear functions of P (rel.4c), data from [3] and [32]. The important point to note is that ΔVm and ΔRm extrapolate to zero at the same characteristic pressure P* = 1.7 to 1.9 GPa as expected from the R ~ V conjecture (rel.4) and in good agreement with the P* values deduced from the FST-Is.

Potassium and Cesium

Potassium

The relative resistivity data of Bridgman, Figure 5 of reference [1], are reported in Figure 5. The fit of the V-T-P data (plain lines) with the m-VW EOS given in reference 17] leads to the characteristic parameters: P* = 1.7 GPa , V^*/V_0=0.32. The fit of the R-T-P data (plain lines) with the m-VW EOS leads to P* = 0.4 GPa , R^*/R_0= 0.04 (R_0 value at 0°C and P=0). The FST-Is is observed, the convergent point (P* ~ 0.6 GPa, R^*/R_0 ~ 0.01) is the same for solid (25 and 60 °C) and liquid (95, 130, 165 °C). Na and K present a similar behavior (Figure 3 and Figure 5). In the inset of the Figure 5 one has reported the resistivity jump ΔRm/R0 at the melting transition as function of the pressure (data from Bridgman), R0 is the reference at 0 °C and P=0. As for Na the R ~ V conjecture is verified, the tangents to the ΔRm/R0 curve cross the P axis at P* ~ 1.2 GPa not far the value of P* determined by the others methods.

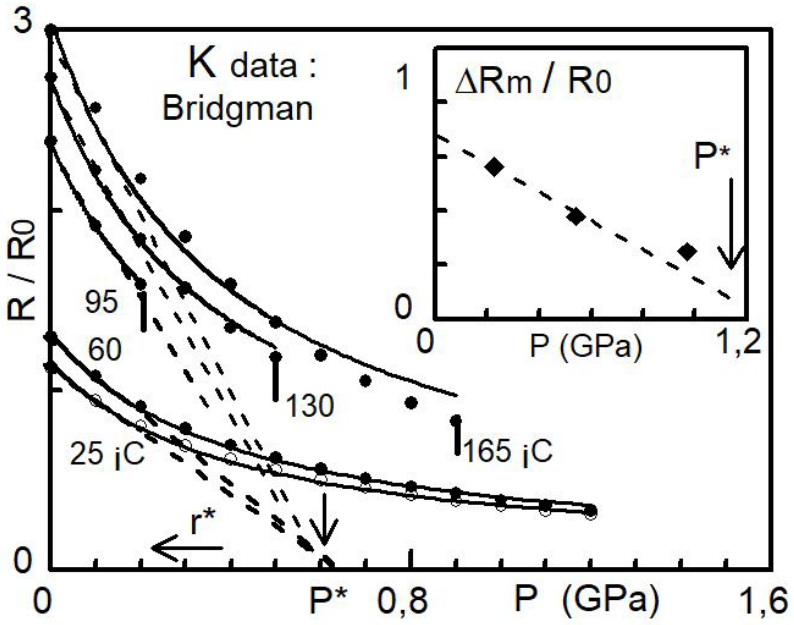

Figure 5: Relative resistivity of Potassium at different temperatures as function of pressure, data from Bridgman [1]. Solid state at 25 and 60 °C, liquid state at 95, 130, 165 °C. R0 is the resistance at 0 °C and P=0. Vertical bars indicate the resistivity jumps at the melting temperature. Plain lines are the mVW-EOS fit with the same characteristic pressure P*= 0.4 GPa and R*/R0=0.04. The tangents at P=0 to the EOS curves (dashed lines) form a Fan Structure (FST-Is) with the same characteristic pressure P* = 0.6 GPa. Insert: Resistivity jump ΔRm/R0 versus pressure at the melting transition deduced from the isotherms at 95, 130, 165 °C

Cesium

The pressure dependence of the resistivity at various temperatures has been reported by Jayaraman et al [34]. Cs present 4 crystalline phases (I to IV). In the domain 30 < P (GPa) < 42.5 the melting curve, II→liquid, has a negative slope $(dTm/dP)_{II}$ = -13 K/kbar and in the domain 42.7< P (GPa) < 55 the melting curve, IV→liquid, has a positive slope $(dTm/dP)_{IV}$ = 11.2 K/kbar. At 120°C the melting of phase II occurs at P=40 kbar and re-crystallization to phase IV at 45 kbar. The corresponding changes of volume in cc/mole are $(\Delta Vm)_{II}$ = -1.99 and $(\Delta Vm)_{IV}$ = 1.72, and the change of relative resistivity: $(\Delta Rm/R0)_{II}$ = -10 and $(\Delta Rm/R0)_{IV}$ = 9, see Fig.3 and Table 2 of their reference. The relation between the ratios ΔRm/R0 and ΔVm/V0 at melting of each crystalline phase and dTm/dP is then:

$$(\Delta Rm/R0)_{II} / (\Delta Rm/R0)_{IV} = (\Delta Vm)_{II} / (\Delta Vm)_{IV} = (dTm/dP)_{II} / (dTm/dP)_{IV} = -1$$

the constant ratio, -1, confirms that the resistivity and volume changes at the transition are proportional whatever is the nature of the crystalline phase. As noted by Bridgman ΔRm and dTm/dP have same sign. The temperature coefficients of the relative volume and resistivity $\alpha(V) = (1/V_{ref})\,(dV/dT)$ and $\alpha(R) = (1/R_{ref})\,(dR/dT)$ are compared in Table I. The reference volume of Cs at 270 K is 70 cm^3/mole [33]. The ratios $\alpha(R)\,/\,\alpha(V)$ of alkali metals are of the same order 16 to 24

Mercury

In Figure 6a one reports the relative resistance of liquid Hg at 5 temperatures between 0 and 100 °C as function of pressure, data from Bridgman, Table IX of ref. [1].

Heavy lines are the fit of the data with the m-VW EOS (R ~ V conjecture, rel.1b). The characteristic parameters are the same for all isotherms: P*=1.6 GPa, R^*/R_0=0.4 to 0.5. In the figure one verifies that all the curves can be superposed by simple translation ΔP as indicated by the double arrows. One compares in table 3 the characteristic parameters P*(V) and P*(R) and the thermal pressures $(dP/dT)_V$ and $(dP/dT)_R$ at constant V and R deduced from the V(T,P) and R(T,P) curves (columns V and R). The (V) data have been deduced from the works of several authors, see ref. [17] and [27], recent work of Ayrinhac et al [35] by acoustic velocity measurements between 293 to 513 K are given in bracket. The (R) data are deduced from figure 6a.

P*(X) (GPa)				$(dP/dT)_X$ ($MPaK^{-1}$)			
EOS		FST-Is		x = V or R			
V liq	R liq	V liq	R liq	V α	V β	V liq	R liq
5.2	1.6	4 (3)	1	4	5.3	3.8 (4.2)	2.6

Table 3: Characteristic pressure P*(V) and P*(R) of mercury in the liquid state and in the α and β crystalline states deduced from the EOS rel.1a,b and from the convergence point of the FST to the V(P) and R(P) isotherms. Thermal pressures $(dP/dT)_X$ at low pressure determined at constant volume (V) and constant resistance (R). See references in text

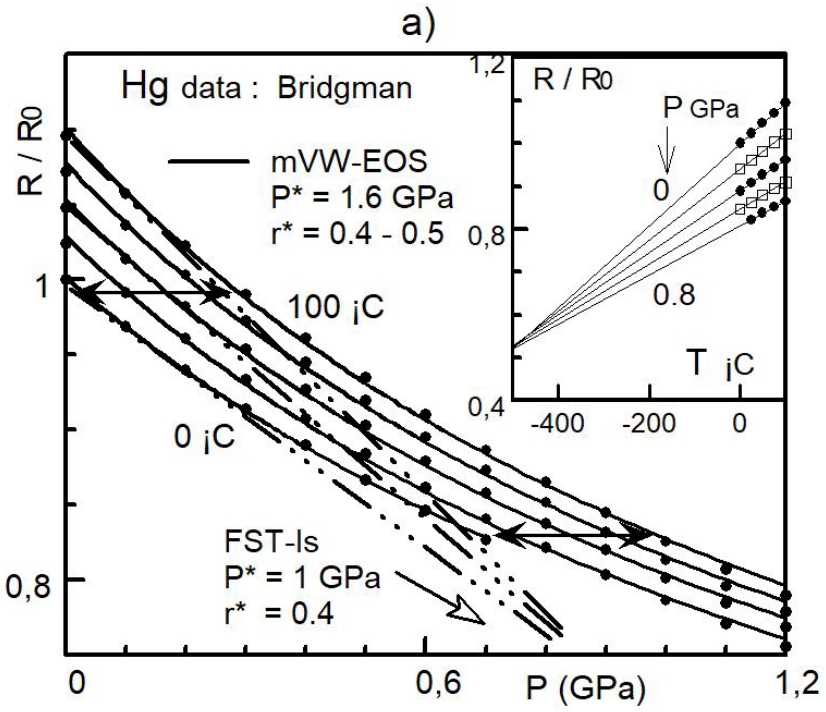

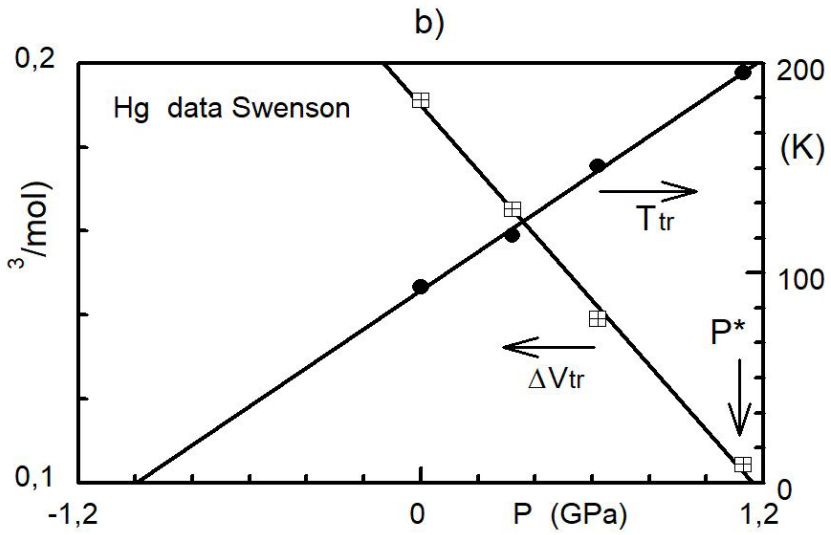

Figure 6: a) Relative resistance of mercury at constant temperature, from 0 to 100°C per step 25 °C. Data from Table IX of ref. [1]. Heavy lines are the m-VW EOS fit, rel.1b, the characteristic parameters P* and $r^*=R^*/R_0$ are indicated. The tangents to the isotherms at P=0 (dashed lines) form a Fan Structure (FST-Is); the convergent point is P*, $r^*=R^*/R_0$, see text. Double arrows are the constant translation ΔP to superpose the two isotherms at 0 and 100 °C. Insert: isobars at pressures from 0 to 0.8 GPa , per step 0.2 GPa.

b) Temperature T_{tr} and volume jump ΔV_{tr} (cm3/mol) at the crystalline transition β → α of mercury, data from Swenson [27]. The characteristic pressures P* deduced from the Clapeyron relation and from the m-VW EOS, rel.1a and 4a, are indicated

From the above Table one concludes that:

a) from the experimental isotherms V(P) and R(P) the P* values determined by the different methods (EOS fit, FTS-Is) are of the same order: P*(V) = 4 to 5,2 GPa and P*(R) = 1 to 1,6 GPa. This small difference is very probably due to the accuracy of the data to the different approximations used and to different calibration of the pressure.

b) The thermal pressure $(dP/dT)_V$ of the α and β solid phases and liquid phase are respectively 4, 5.3 and 3.8 MPa K^{-1}, see ref. [17]. The thermal pressure $(dP/dT)_R$ = 2.6 MPa K^{-1} of the liquid is about equal to $(dP/dT)_V$ = 3.8 MPa K^{-1}. The R ~ V conjecture, rel. 4f, is then verified.

c) The transition temperature Ttr (α → β) occurs between 90 to 200 K for P<1 GPa. The slope of the transition curve is dP/dTtr = 4.5 MPaK^{-1}, this value deduced from the V(P,T) data of Swenson [27] is about the thermal pressure $(dP/dT)_V$ =3.8, 4, 5.3 MPaK^{-1} of the liquid α and β phases (see Figure 9 of ref. [17]). The Slater conjecture is then verified.

In the inset of the Figure 6a the isobars R(T) at 5 pressures are drawn, from 0 to 0.8 GPa step 0.2 GPa (data from Bridgman). As P<P* linear variation is observed and these FST-Ib (straight lines) converge to the point T*~ -500 °C , R*/R0~0.55. In figure 9a of ref. [17], we have reported the FST of the isobars V(T) of Kuchhal et al [36]. The convergent point is T* ~ -500 °C , V*/V0 ~ 0.9. There is a very good agreement in the negative values of T* deduced from the V and R data of the different authors also one concludes that the ratios V*/V0 and R*/R0 are of the same order (factor 1.5).

In Figure 6b is given the transition temperature Ttr and the volume jump ΔVtr of the crystalline transition β → α at low temperature 70 < T < 200K as function of P, data from ref. [27]. As predicted by rel.5, Ttr and ΔVtr vary linearly with P at low pressure. ΔVtr extrapolates to 0 at P* and Ttr extrapolates to 0 K for the negative pressure - P^*.

Lead

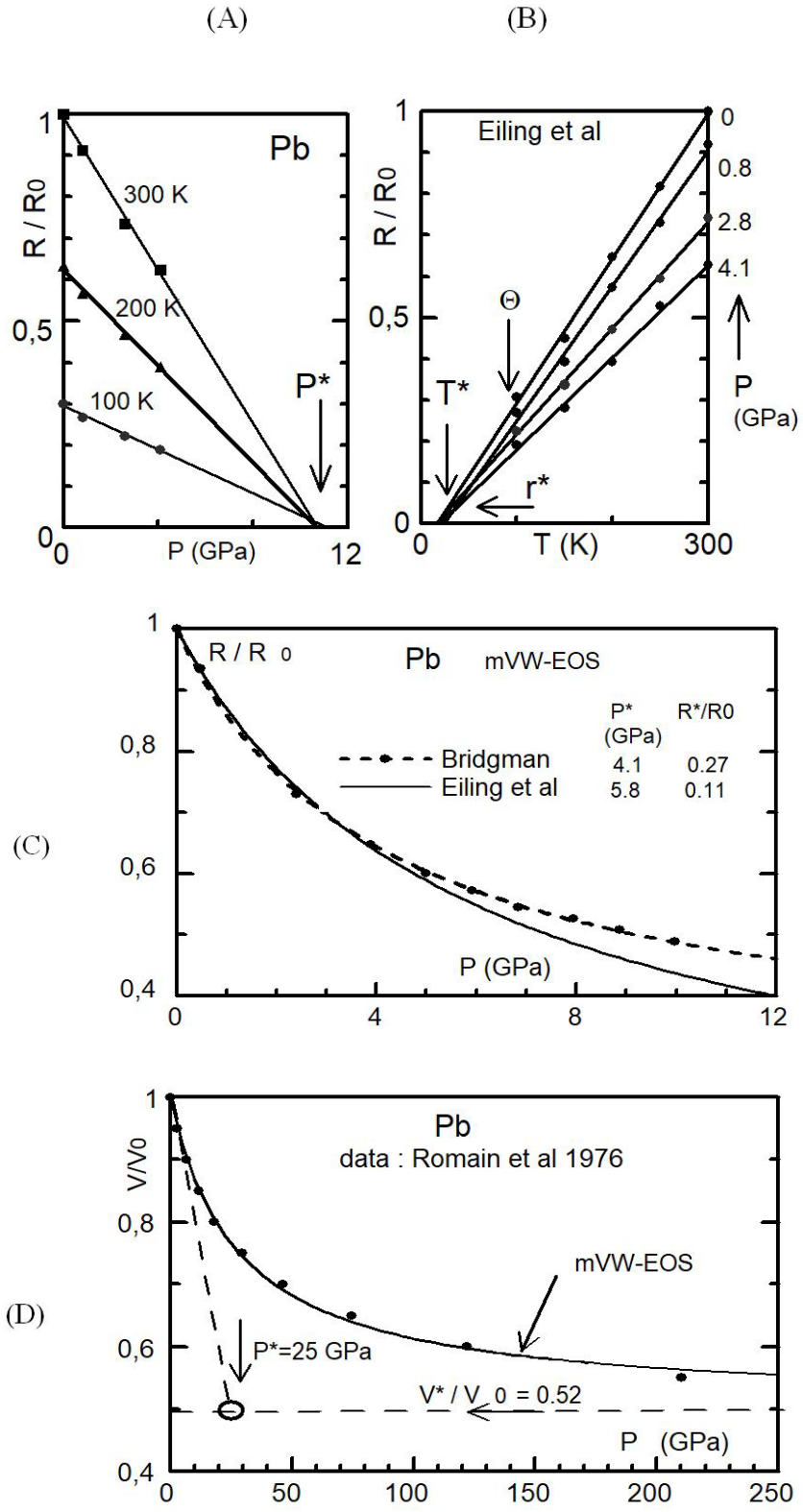

Figure 7: Relative resistivity R/R_0 and volume V/V_0 of Lead as function of pressure and temperature. a,b) isotherms and isobars resistivity, data from Eiling and Schilling (Figure 5 of ref. [37]). c) Isotherm R/R_0 versus P at 300 K, data from Bridgman [1] and recalibrated by Eiling et al see text. d) isotherm V/V_0 versus P at 300 K reported by Romain et al at (from Fig.1 of ref. [39]). In c) and d) lines are the fit of the m-VW EOS, the characteristic parameters P* V* and R^*/R_0 are given

One gives in Figures 7a,b the relative resistivity isotherms at 3 temperatures and isobars at 4 pressures, data from Eiling and Schilling [37]. From these data one concludes that the FST-Is is observed (Figure a), the characteristic pressure is P*=10 GPa, not far from the value P*=7.5 GPa deduced from the data of Bridgman (FST-Is given in Figure 2b). The FST-Is in the high (273-373 K) and low (100-300 K) temperature domains and for low pressure (P<P*) lead to the same characteristic pressure P* , see Figure 2b and Figure 7a.

In Figure 5 of their paper Eiling et al. reported the isobars R(T) for 0<P<4 GPa in the domain of temperature 40-300 K. All Isobars for P<P* are linear functions of T and no change of behavior is observed at the Debye temperature 89 K. In Fig.7b their R(T) values are given for only 5 temperatures, the convergence to point is T*=25 K and r*~ 0. Aleksandrov et al [38] observed same linear isobar at P=0 with the same extrapolated temperature T*, see Figure 1a.

In Figure 7c one compares the resistivity of Pb at 300 K measured by Bridgman and Eiling et al, the data come from Figure 2 of reference [37]. The difference between these two curves could be due to the calibration of the pressure; Eiling et al used the various crystalline phases transitions of Bi and Tl to calibrate the pressure between 2.5 and 7.3 GPa. The m-VW EOS fits lead to somewhat different characteristic parameters P* and R^*/R_0 given in the Figure.

In Figure 7d one gives the relative volume at 300 K versus P, plain circles are the experimental points determined by shock wave experiments, see Figure 1 of reference [39]. The fit with the m-VW EOS leads to the characteristic parameters P*=25 GPa and $V^*/V_0 = 0.52$ about 3-5 times the values deduced from the FST-Is (Eiling et al: P*=5.8 GPa and $V^*/V_0 = 0.11$). This difference between the values determined in a T and P domain (EOS fit and FST-Is) and those determined at one temperature and at high pressure should not be astonishing. The determination of the volume by wave propagation rests on various assumptions, see ref. [40] , the comparison of the experimental curves V(P) determined by the various methods has never be discussed to the best of our knowledge.

Iron

In Figure 6 of ref. [17] one has shown that the characteristic pressures, P*, PTm , PB, PG, deduced from the m-VW EOS , the P variations of the melting temperature Tm , the bulk and shear moduli (B, G), are not different, 60 to 68 GPa. The Bridgman isotherms R(P) at 0 and 100°C at low pressure (P<2 GPa) are reported in the inset of Figure 2a. In the figure it is shown that the linear extrapolation of these two isotherms (FST) in the high pressure domain converge at P*= 40 GPa not far from the P* EOS value. This author has not studied this metal at low temperature. Isobars R(T) at P=0 from 2 to 300 K have been reported by several authors. In Figure 1c the data at two pressures are given: triangles, data at P=0 from the Meaden review, full circle data at 25 GPa of Shimizu et al [41]. Only the data of these authors at different T, per step 25 °K, are given. In Fig. 1d the data of these authors are given as function of P for 4 temperatures, the FST to the isotherms R(P) is clearly observed. From the isobars and isotherms of Fe given in Figures 1c and Figure 2a one concludes that:

a) Between 100 and 300 K the two isobars R(T) at 0 and 25 GPa are linear function of T, which converge to the point (T*=50 K, R*/R0 ~ 0.05).

b) At low temperature below the temperature T^*_0 ~ 100 K the resistivity scales according to the empirical relation $R \sim T^n$ where n is about 3.2 very different from the exponent 5 predicted by the (Umklapps) theoretical model, such departures from this law is usually observed [12].

c) There is a very good agreement between the R-T-P data of Bridgman at high temperature (0 < T < 100 °C) and those of Meaden and Shimizu at low temperature (-200 < T < 0 °C); the FST to the isotherms R(P) (Figure 1d and Figure 2a) have same convergent point (P*, R*/R0). The pressure P* deduced from the R-T-P and V-T-P data (m-VW EOS (rel.1) are very similar, 60 to 68 GPa.

These properties confirm the R ~ V conjecture.

Tin

Babe [41] has shown that the melting temperature $T_m(P)$ of Tin varies linearly with P at low pressure (P<9 GPa), from his data and rel.4a one deduces the characteristic pressure P_{Tm}=16 GPa. From the various EOS used by different authors, see ref. [42], the bulk modulus and its derivative at P=0 are B_0 =50 to 56 GPa and B'_0 =4.8 to 5 then the characteristic pressure of the m-VWEOS (rel.2) is P*(V) = 18 ± 1 GPa. The universal relation P*(V) = P_{Tm} of alkali and transition metals, see table 1 of ref. [17, is verified with a great accuracy.

Zu et al [43] have measured the resistivity of Sn (and Sn-Sb alloys) between 100 and 1100 °C. The resistivity R_S and R_L of Sn (Tm =240 °C, Θ =200 K) in the crystalline and liquid states are linear function of T. The temperature coefficients of resistance (or resistivity) and volume at P=0 deduced in both domains are reported in table 4. Also are given the relative jumps ΔVm/Vs and ΔRm/Rs at the melting temperature under atmospheric pressure. From this Table one concludes that the V~ R conjecture is not perfectly verified: a) the temperature coefficients $\alpha_l(V)$ and $\alpha_l(R)$ are of the same order (factor 2). b) the relative jumps $\Delta Vm/V_L$ and $\Delta Rm/R_s$ are also of the same order (factor 5). However one notes that the coefficients $\alpha_s(R)$ is higher than $\alpha_s(V)$ (factor 10), this is very surprising. It is obvious that such relation between the temperature coefficients α must be studied in the same sample (purity) using the same experimental methodology (same thermal history, same isotropy and dimensions of the crystalline domains in the solid state). In the following one will verify that in Sn mono-crystals for 0<T<90°C the P*(R) and P*(V) values are very similar.

P_{Tm} (GPa)	P*(V) (GPa)	P*(R) (GPa)	$\alpha_l(V)$ ($10^{-3}K^{-1}$)	$\alpha_s(V)$ ($10^{-3}K^{-1}$)	$\alpha_l(R)$ ($10^{-3}K^{-1}$)	$\alpha_s(R)$ ($10^{-3}K^{-1}$)	$\Delta Vm/V_S$	$\Delta Rm/R_S$
16 rel.2	18 rel.1	12 Rel.1	0.1 a)	0.06 b)	0.44 c)	5 4.6 c) d)	0.2 e)	1 c)

a) Bar'yakhtar et al [44] , b) Lide [45] , c) Zu et al 43] , d) Bridgman [3] , e) ref. [46]

Table 4: Temperature coefficients (α_l , α_s) of the volume (V) and resistivity (R) of Sn in the solid and liquid states. $\Delta Vm/V_s$ and $\Delta Rm/R_s$ are the relative jumps of volume and resistivity at the melting temperature under ambient pressure

Gold, Copper

Gold

In figures 8a the temperature variations (0 < T < 2000 K) of Vs and Rs of solid Au (fcc) at ambient pressure are given, in figures 8b,c Vs and Rs are compared to VL and RL. Experimental V data come from Kaptay, figure 2 of ref. (19). R data come from Matula table 5 of ref.(10) and from Berrada et al (figure 2 of ref [47]. Kaptay showed that the T-dependence of the molar volume of crystalline and liquid Au (in cm^3/mol) at ambient pressure are given by the rel.2 and 7:

$$Vs = V^* + 7.028\times10^{-5}\, T^{1.27} \quad ; \quad V^* = 10.113 \quad T < 1337\ K \qquad (7a)$$

$$VL = V^* + 8.58\times10^{-4}\, T \quad ; \quad V^* = 10.15 \quad T > 1337\ K \qquad (7b)$$

It is important to remark that the extrapolated volumes VS and VL at T=0 in both temperature domains (figure 8b) is the characteristic parameter V* of the m-VW relation. This characteristic volume can be found by various methods: the FST to the isotherms to the V(P) curves and by the fit of the V(P) curves with the EOS rel.1b

The resistivity data (μΩ−cm) of Matula (see table IV of ref.(10) and Berrada et al, see at ambient pressure follow similar relations:

$$R_s = 0.07 + 16\times10^{-4}\, T^{1.27} \; ; \; R_L = 0.022\, T \; ; \quad C^* > 0.999 \qquad (7c)$$

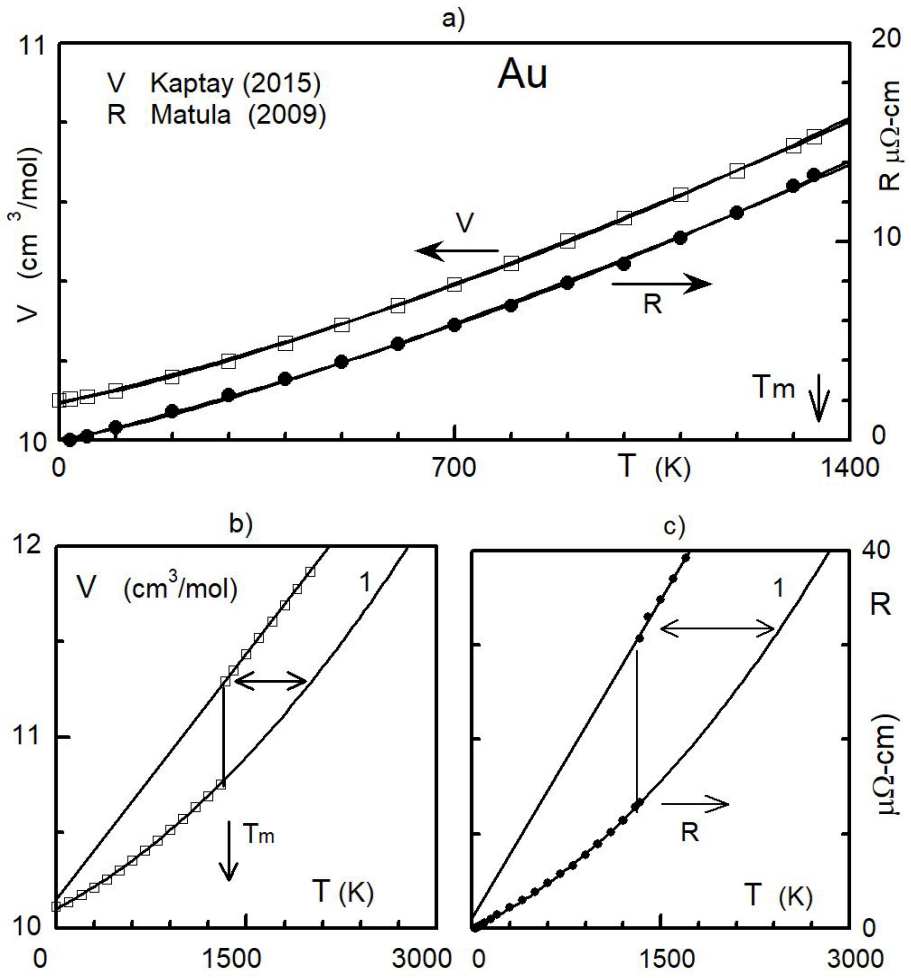

Figure 8: Variation of the volume and resistivity of gold at ambient pressure versus temperature. The data come from Kaptay and Matula, see text. a) crystalline state: fit curves V (rel.7a) and R (rel.7c). b) and c) same fit curves extrapolated above and below the melting temperature. The linear V and R curves of the liquid state can be superposed (double arrow) with the corresponding fit curves of the solid state, lines 1.

In figure 8c the data of these authors are fitted with these relations. One concludes that the ratios of the thermal components v = V-V* and r = R-R* of the solid and liquid states are of the same order at any temperature:

$$v_L / r_L = 0.03 \;;\; r_L / r_S = 0.04 \;;\; (V\ cm^3/mol, R\ \mu\Omega\text{–}cm) \quad (8a)$$

$$v_L / v_s = 1.75 \;;\; r_L / r_s = 2.2 \quad (at\ T_m) \quad (8b)$$

The correlation factors C* are excellent, the residual resistivity R*(T=0) = 0.07 can be neglected. Finally it must be noted that the characteristic pressures P* deduced from the fit of the V(T,P) and R(T,P) data with the EOS rel.1a,b are of the same order, see ref. [48,49].

Copper

The variation of the volume deduced from Kaptay work, Table 3 of ref. (19), is given by the relation: Vs =7.04 + 3159 T^n cm^3/mol, n =1.355. R(T) data of Matula (table 2 of ref.(10) can be put on the same form : RS = 5.95 T^n μΩ–cm, n =1.355. The correlation factors of both fits are better than 0.997. From the data of these authors above and below Tm one deduces the ratios of the thermal components v = V-V* and r = R-R* of the solid and liquid states at Tm:

$$vL / vs = 1.74 \;;\; rL / rs = 2.07 \quad at\ 1358\ K \quad (8c)$$

In conclusion the R ~ V conjecture is perfectly verified in Au and Cu.

Phosphorus

The relative resistivity R/R0 of black Phosphorus in the solid state (0 <T<100°C and 0<P<1.2 GPa) is given in Figure 9, the data come from Table XVII of the Bridgman review [1]. Plain lines are the fit with the m-VW EOS with the same characteristic values, P* = 0.4 GPa and r*= R^*/R_0 ~ 0. At low pressure the FST-Is is observed and the convergence point of the tangents at P=0 is P*=0.4 GPa and r*=0.02 in total agreement with the EOS fit value. At 0°C the α – β transition is observed at P = 0.6 GPa, and the two different parts of the isotherm curve are fitted by the same EOS with only a different initial V_0 values. In the Bridgman classification black P is a "normal" metal, the resistivity decreases when P increases. But unlike most of the CM materials phosphorus has a abnormal behavior at low pressure, P<0.8 GPa; the resistivity decreases with increasing temperature then if the R ~ V conjecture is verified, V should decrease with P. This is unphysical excepted if a phase transition with a negative volume jump exists in the domain of measurements (typical example of water).

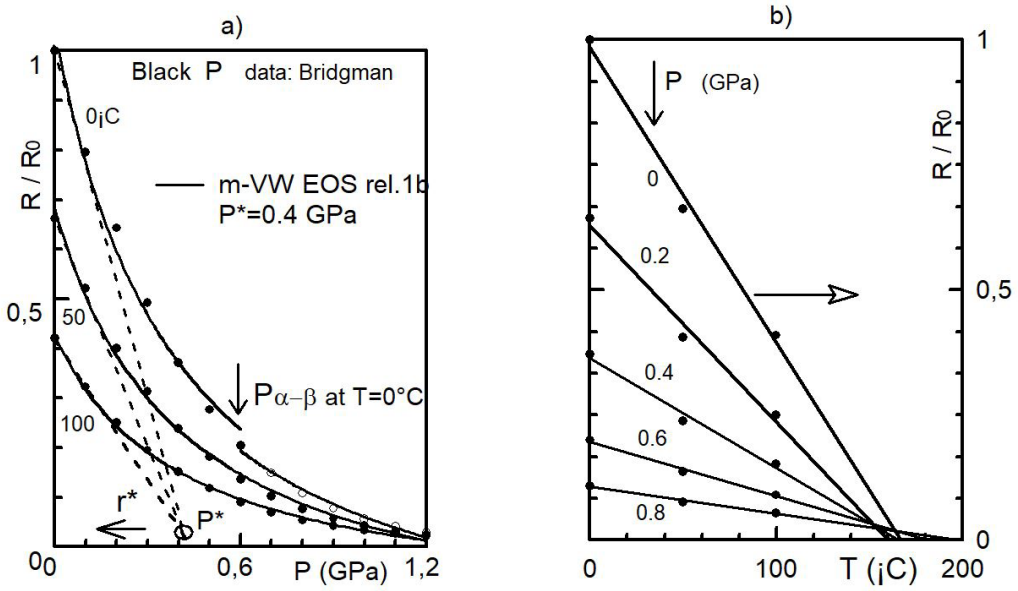

Figure 9: Relative resistivity of black Phosphorus versus pressure and temperature, data from Bridgman [1]. a) Heavy lines are the mVW-EOS fits with P* = 0.4 GPa and R*/R0 =-0.1. The tangents (FST-Is: dashed lines) to the experimental isotherms at P = 0 form a fan structure with the convergent point at P*. The isotherm at 0 °C present a discontinuity at the α-β crystalline transition, Pα–β ~ 0.6 GPa. b) isobars: data from Figure (a) lines are linear regressions

Clark [50] and Monaco et al [51] had described the complex (metastable) phase diagram of white and black Phosphorus. The important point to note is that in the T and P domain studied by Bridgman the transition orthorhombic to rhombohedric structure is observed. According to Monaco et al the transition temperature T_{tr} between these two structures of black Phosphorous decreases with P, the slope of the transition curve dP/dT_{tr} is negative about -6 to -10 MPa K^{-1}. The slope $(dP/dT)_R$ at constant resistivity deduced from figure 9a is negative about - 4 MPaK^{-1}. One concludes that the conjectures of Bridgman and Slater rel. 1b and 4e are verified

$$\left(dP/dT\right)_V = \left(dP/dT\right)_R = k_{tr}\frac{dP}{dT_{tr}} \quad ; \quad k_{tr} \approx 1 \tag{9}$$

Crystalline and Amorphous Alloys

Stainless steels

One finds in the reviews of Ho et al [52] and Desai et al [53] the V-T and R-T properties of 9 stainless steels sheets AISI at ambient pressure. In most of these crystalline alloys the resistivity ρ and the linear thermal expansion $\Delta L/L_0$ is linear with T between 50 K and 600 K. Above 600 K up to the melting temperature the curves present some curvature toward the T axis, this would be due to the development of a austenite structure on heating. In AISI 410 and 430 the linear variation of ρ(T) and $\Delta L/L_0$(T) are observed up to 1000 and 900 K. At 300 K the temperature coefficients at constant P of these two alloys are:

$$\alpha_{(V)} = \frac{1}{V_0}\frac{\Delta V}{\Delta T} \approx 3\frac{1}{L_0}\frac{\Delta L}{\Delta T} = 3.6\,10^{-5}\ K^{-1} \quad ; \quad \alpha_{(R)} = \frac{1}{\rho_0}\frac{\Delta \rho}{\Delta T} = 1.4\,10^{-3}\ K^{-1} \qquad (10)$$

The V ~ R conjecture is observed, the ratio α(R) / α(V) = 30 is constant between 200 and 800 K its value is between the Na and Pb values (24 and 49, see table 4) . It must be noted that the formation of stainless sheets of steels (by compression, drawing, melt spinning…) can produce some orientation of crystalline structure in the sheet, the α_V value deduced from the thermal linear expansion is then very crude.

Amorphous metallic alloys

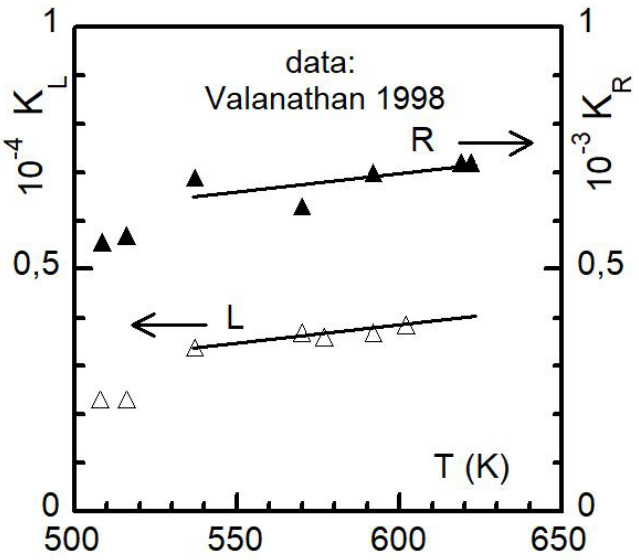

Figure 10: Glassy metallic alloy ($Fe_{40}Ni_{60}B_{20}$) annealed during different times (t) at different temperatures below Tg. K_L and K_R are the slopes of the expansion L and resistance R curves versus the logarithm of the aging time at constant temperature, $K_L=\Delta L/L_0$(ln t) and $K_R=\Delta R/R_0$(ln t) data are deduced from the work of Valanathan, [56]

Allias et al [54] had measured at different temperatures the electrical resistivity of three series of alloys in form of ribbons (Fe-B-Si, Fe-Ni-Mo-B, Fe-Cr-B) of different thickness prepared by melt spinning. The relative resistivity variation $\Delta\rho/\rho_0$ varies linearly with T between 293 K to 345 K , the slope of each series decrease when the thickness decreases. This is what is expected if the R ~ V conjecture is verified. Also Kelton et al [55] had studied the effect of densification on the resistivity behavior of various other metallic glasses. In annealed samples they noted the very similar kinetics of resistivity and viscosity relaxations. To our knowledge only Valanathan [56] has compared the volume and resistivity of a metallic glass ($Fe_{40}Ni_{60}B_{20}$) as function of temperature and annealed time at ambient pressure. The relative dimension $\Delta L/L_0$ and resistivity $\Delta R/R_0$ vary linearly with the logarithm of aging time at constant T between 530 K and 620 K (see figure 4.3 and figure 4.4 of ref. [56]). The slopes $K_L = d\Delta L/L_0)/dln(t)$ and $K_R = d\Delta R/$

R_0)/dln(t) are reported versus T in figure 10. A discontinuity is observed at 530 K, whose origin is unknown. Below and above this temperature these slopes are constant. One recalls that in aged isotropic and oriented amorphous polymers [18,31] the slope K_V is also a constant independent on the aging temperature. Noting that $\Delta V/V_0 = 3\Delta L/L_0$ one concludes that $K_R \sim 6\ K_V$. These similar aging properties (volume, viscosity, resistivity) of the amorphous metallic alloys is a consequence of the R ~ V conjecture (m-VW EOS) and of the VFT law (rel.6).

Supraconductors with Quasi-1D and -2D structure

Various alloys and organic conductors of these types have been studied, the interest of these alloys is that the structure is somewhat intermediary between the 3D-crystalline structure and the amorphous structure. One gives here four examples:

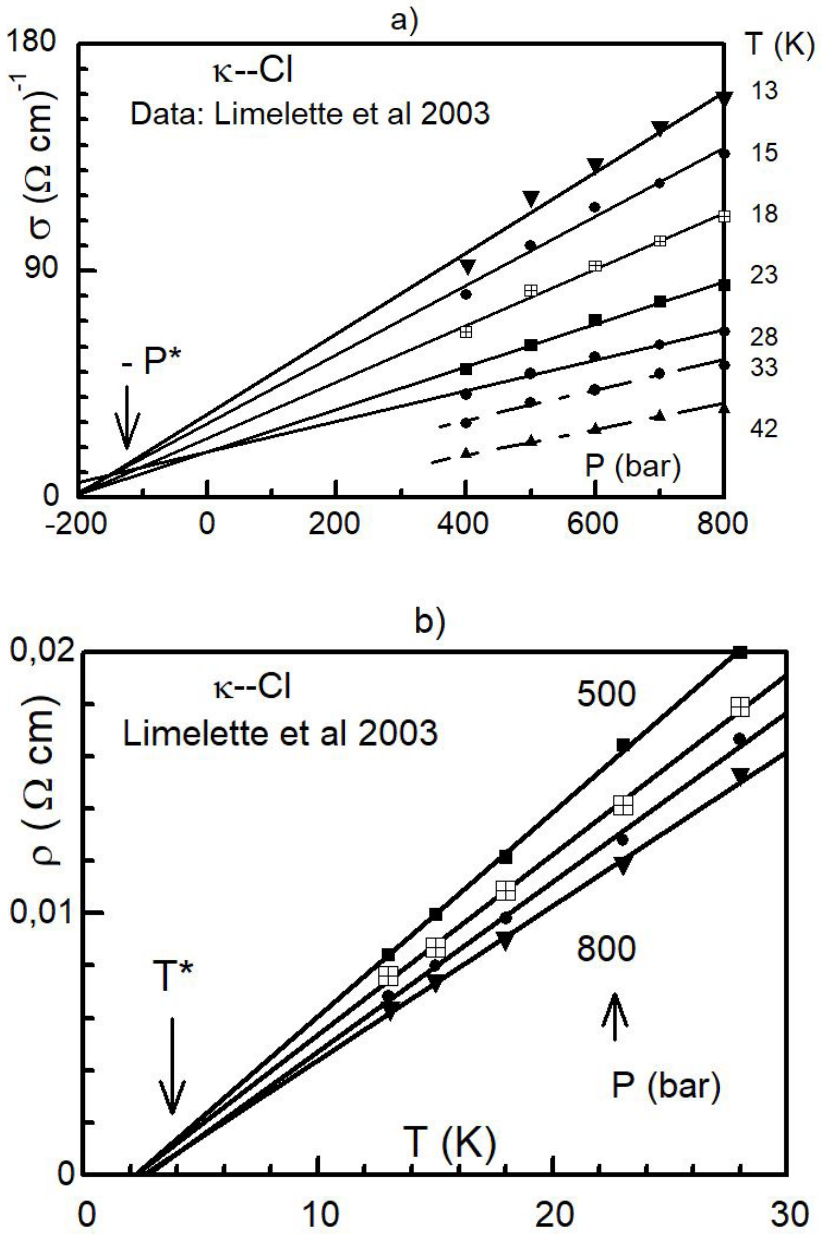

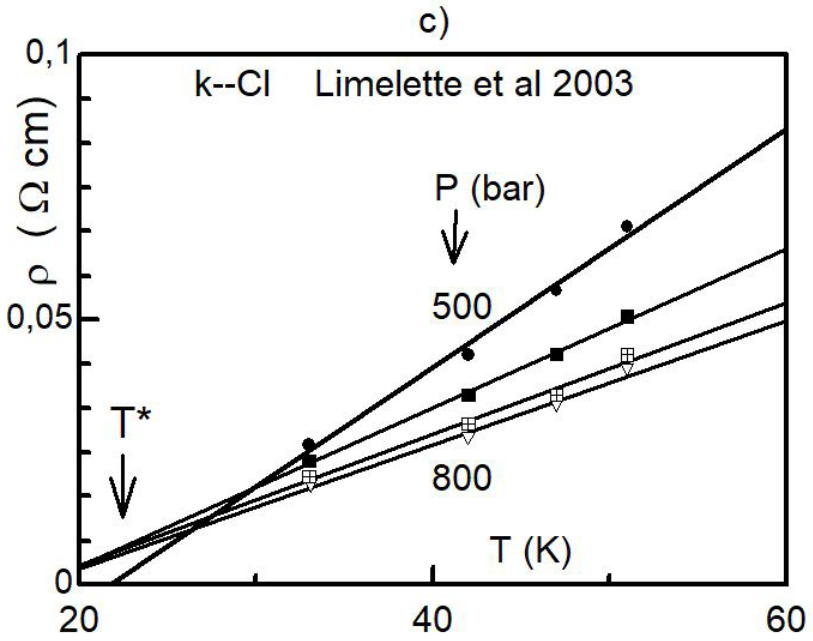

Figure 11: Conductivity σ(P) and resistivity ρ(T) of the k-Cl organic salt, data deduced from Fig.2 of Limelette et al [52] . Plain lines are linear regression. a) FST-Is in the domain 400<P<800 bar and 13<T (K)<30 b) FST-Ib in the Fermi-liquid domain, T <30 K. c) FST-Ib in the Bad-metal domain, T >30 K. In b) and c) isobars at 500, 600, 700 and 800 bar

κ-Cl salt. Limelette et al [57] have studied the conductivity σ of a layered charge-transfer salt κ-(BEDT-TTF)$_2$Cu(N(CN)$_2$)Cl which displays a complex phase diagram T(P), the superconducting phase is observed below 300 bar and 25 K. Four transport regimes have been identified. The Bad-metal and the Fermi-liquid regimes are separated by the transition line Tmet (K) =18+0.4 Pmet (bar) in the domain 300<P<800 bar. Above 400 bar in the Fermi-liquid region 10<T<40 K, the conductivity σ vary linearly with P, see their figure 2. In figure 11a one reports their data σ(P) for 5 temperatures from 13 to 28 K. It is important to note that the 5 isotherms curves present a Fan Structure (FST-Is); the fits of all these data (T<33 K) with the linear relation $\sigma = \sigma_0(1+P/P^*)$ lead to the characteristic pressure P* = 90 ± 10 bar ; the mean correlation factor Rc been between 0.98 and 0.99. The resistivity is then $\rho = 1/\sigma = \rho^* P^*/(P + P^*)$ and the R(T,P) EOS rel.1b is verified.

In figure 11b,c one reports the isobars ρ(T), below and above the transition line, Tmet ~ 30 K, the data ρ(T)=1/σ(P) are deduced from figure 2 of reference [57]. Each isobar is fitted by a linear regression, the correlation factor Rc of each fit is better that 0.99. Isobars form a Fan Structure (FST-Ib) in each temperature domain, but the extrapolated convergence points, T* ~ 3 (T<30 K) and T* ~ 20 K (T>30 K), r* ~ 0, are not well defined. One note that the T* value of the Fermi-liquid region is not far of the Tc of the superconducting phase.

$CeRhIn_5$ and $K_2Cr_3As_3$ studied by H. Hegger et al [58] and Bao [59]. These compounds, superconductors below 2 K and 6 K, have quasi-2-dimensional and quasi-1-dimensional structures. In both alloys a linear temperature dependence of resistivity is observed in a broad temperature range above the superconducting temperature up to 300 K.

Cuprates, These materials have been studied by various authors, references are found in the recent reviews of Doiron-Leyraud et al [60] and Legros et al [61]. These last authors have shown that once the superconductivity is suppressed by a magnetic field the resistivity has a perfect linear T dependence above and below the supra-conductivity temperature, see figure 2b of ref. [61]. The T variations of the volume of these different alloys, submitted or not to a magnetic field, has not been measured by the authors, obviously one thinks that the volume varies linearly with T as observed in crystalline and glassy materials, then the R ~ V conjecture would be verified above and below T_C in the non-superconducting state (in presence of magnetic field).

Hydrogen

In figure 17 of reference [17] we have reported the relative volume at 300 K of H2 versus P, data of Anderson et al [62] at low pressure (T= 4.2 K, 0 <P< 2.5 GPa) and of Jiuxun et al [63] at high pressure (2<P <600 GPa). The Generalized Modified Van der Walls EOS :

$$V / V_0 = a_3 + a_1 / (1 + P / P_1^*) + a_2 / (1 + P / P_2^*) \quad (11)$$

discussed in ref. [17] applies for materials which present weak inter-molecular and strong intra-molecular interactions as H2 and polymers. V_0 is the extrapolated volume at P=0. For H2 the fit with the experimental data with the gm-VW EOS leads to the characteristic parameters: P_1^*= O.38 GPa , P_2^* = 26 GPa , a_1 =0.51, a_2 =0.32, a_3 =0.1 . It has been noted in ref. [17] that in the low pressure domain, P<15 GPa, the characteristic pressures P_{C33} =0.3 GPa and P_B =0.6 GPa deduced from the P derivative of the elastic C33 and bulk B moduli are in good agreement with the EOS value P_1^* . In fig. 12 only the data of Jiuxun at high pressure at 300 K are reported (P >> P_1^*). The fit with the gm-VW EOS leads to somewhat different characteristic parameters P_2^* ~ 50 to 75 GPa and V*/V0=0.06. In the figure one verifies that the tangent to the isotherm V(P) cross the horizontal dashed line V*/V0=0.06 at P*= P_2^* ~ 75 GPa, this is the general property deduced from the m-VW EOS and observed in various materials with one type of interaction. In solid and liquid CM this pressure is T independent [17], then one expects that this property, consequence of the FST to the isotherms V(P), is also verified. Weir et al [64] had measured at 20 K the resistivity of H2 and D2 submitted to shock compression 90<P<180 GPa. In the inset of figure 12 their R data (in linear ρ scale) are reported versus P. Below 120 GPa the resistivity (Ω-cm) can be approximated by a linear function of P: ρ (Ω□cm) = 8.8 - 0.083 P (GPa), which lead to P* ~ 100 GPa for ρ* ~ 0. Above 120 GPa the saturation resistivity ρ* is about 500 μΩ–cm the value of a metallic fluid. This pressure is of the order of P_2^* the characteristic pressure deduced from the gm-VW EOS at high pressure, a typical value of liquid metals. From the comparison of the V(P) and R(P) curves one concludes that the R ~ V conjecture is verified, however it should be necessary to verify that the temperature behaviors (FST-Is) of volume and resistivity in the liquid and solid states are similar.

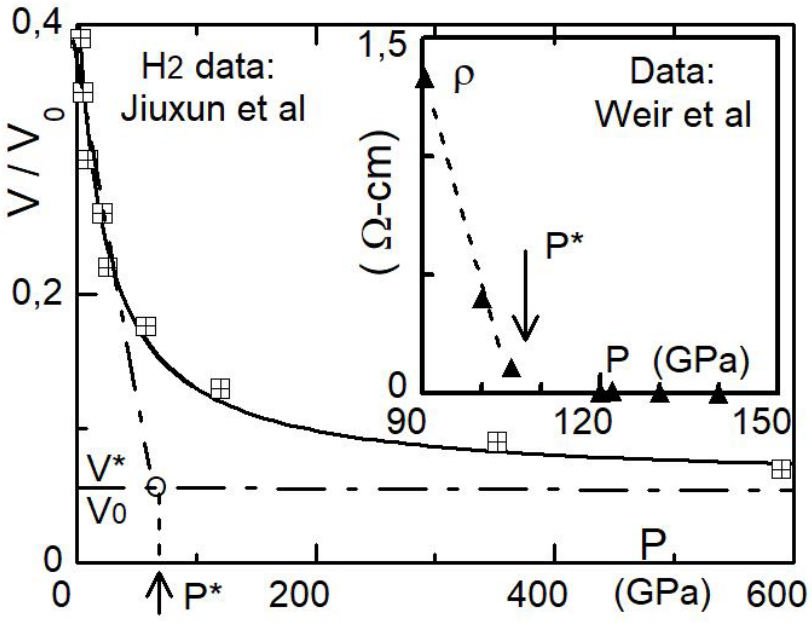

Figure 12: Hydrogen: Variation of the relative volume versus pressure in the high pressure domain at 300 K, data from Jiuxun [63], see Figure 17 of ref. [17]. Heavy line is the m-VW EOS fit with the characteristic parameters P* ~ 70 GPa and V*/V0=0.06. Insert: resistivity versus pressure at 20 K in the high pressure domain, data obtained by Weir et al [64] by shock wave measurements. The two domains above and below P* ~150 GPa are observed. Line is a guide for the eyes

Single crystals; Zn Sn Bi Sr

The metals re-analyzed above are isotropic (polycrystalline or amorphous). For obvious experimental reasons the measurements of size and conductivity of single crystals along the different crystallographic axis as function of P and T are extremely difficult. To our knowledge only Bridgman have reported such resistivity measurements of two "normal" metals (zinc and tin, dR/dP<0) and two "abnormal" metals (bismuth and strontium, dR/dP>0), see Table XIV of ref. [3].

Sn, Zn. In this Table this author gives the relative resistance of Sn and Zn at 0°C and 95°C in a direction making an angle Φ with the long axis of the mono-crystals; for Sn Φ= 11° and 74 ° and for Zn Φ= 7° and 90 ° about parallel (//) and perpendicular (⊥) to the crystal length, the data are reported in Figure 13. According to Knittle [42] these two metals have very similar bulk modulus B and pressure derivative B' at ambient temperature and pressure; Sn: B_0=50 to 56 GPa B'_0=4.8 to 5.5 , Zn: B_0=59,8 GPa B'_0=4.4. The characteristic pressure of the mVW-EOS deduced from B and B' (rel.3) is then of the same order P*~ 18-22 GPa. From Fig.12 one concludes that:

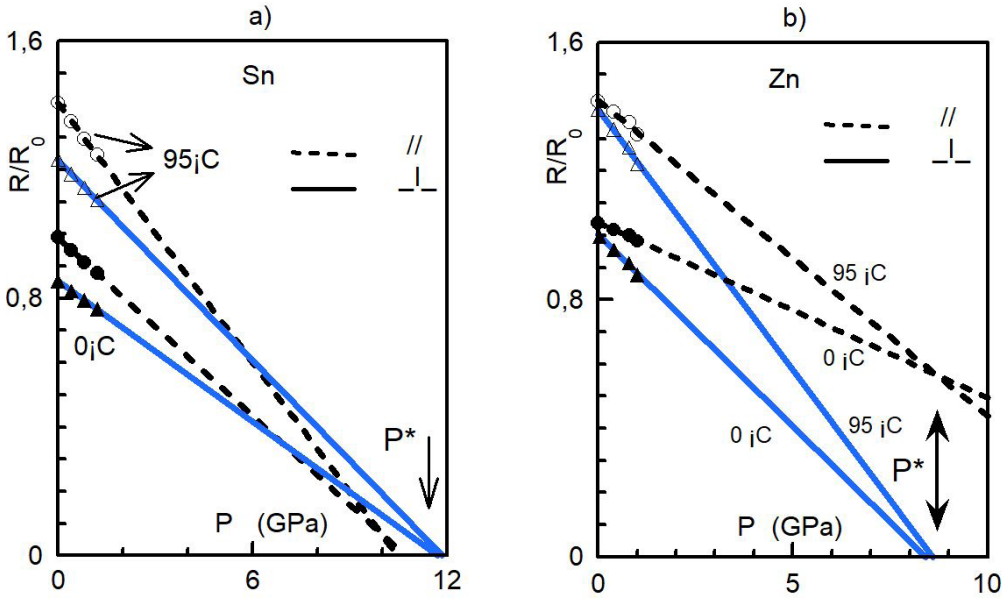

Figure 13: Relative resistance of Tin and Zinc mono-crystals versus pressure at 0 and 95 °C and along two different directions. Angle between the direction of measurement and the crystal axis: Zn, 7° (//) and 90° (⊥) and Sn, 11° (//) and 74° (⊥). Data from Bridgman, see text. For each direction the pressure P*at the convergent point of the FST-Is is the characteristic pressure of the mVW-EOS

a) at constant temperature, whatever is the direction, // or ⊥ , R decreases linearly with P in the low pressure domain (P<P*)

b) As most of the polycrystalline metals, Zn and Sn would present the FST-Is of the R(P) and V(P) curves. Then all the tangents to the two isotherm curves R(P) (// and ⊥) at 0 and 95°C, would converge at the same point (P*, R^*/R_0). One verifies that for these two directions the pressure at the convergence point is the same, 10 – 12 GPa (Sn) and 9 GPa (Zn). This pressure is about the characteristic pressure P* ~ 18 to 20 GPA deduced from the mVW-EOS (rel.3). This property, P* independent on the direction, is not astonishing, we have shown previously that the characteristic pressure P* of any element does not depend on the state, liquid crystalline amorphous, but only its nature.

Bi, Sr. In fig.14a as an example the isotherms R(P) of poly-crystalline Bi, an "abnormal" element (dR/dP>0) are given. The 4 isotherms at 0, 25, 50, 75°C, are deduced from the Bridgman data at low pressure (P<1.2 GPa), figure 23 of ref. [1]. The experimental data can be fitted by a second order polynomial equation and not by the mVW EOS rel. 1b; the FST-Is is not observed however the T-P superposition principle is verified. The arrows in the figure are the constant translation ΔP to superpose the isotherms at 0°C and 25°C and the isotherms at 50°C and 75°C. One verifies that the 4 curves can be accurately superposed by this simple

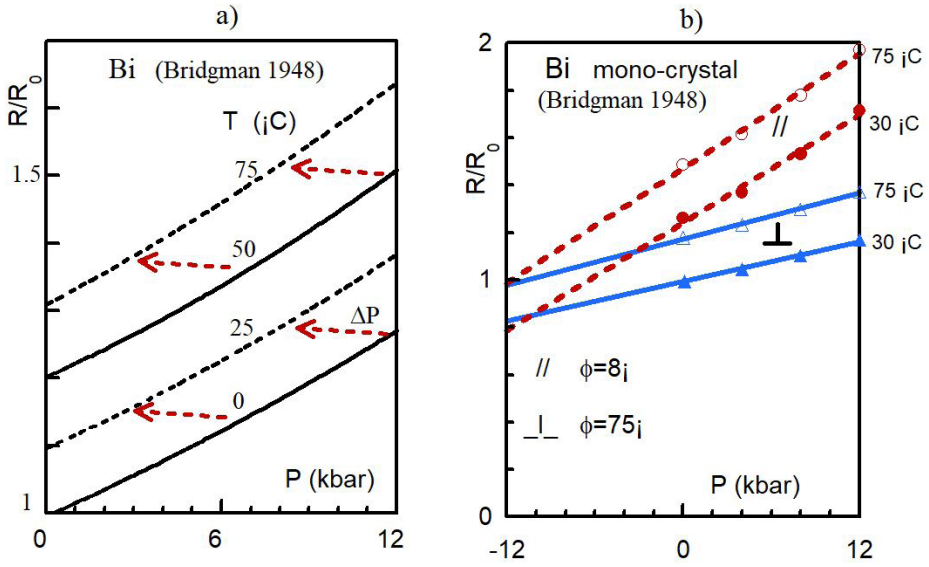

Figure 14: Relative resistance of Bismuth as function of pressure. a) poly-crystalline, isotherms at 4 temperatures. Arrows: translation vector ΔP necessary to superpose two isotherms at T_1 and T_2 (ΔT=25°C). b) mono-crystal, isotherms at 30 and 75°C, measurements in two different directions at a angle φ with the long axis of the crystal. Data from Bridgman [2]

translation ΔP which decreases linearly with ΔT (then with ΔV), $(\Delta P/\Delta T)_R$ = - 18 $MPaK^{-1}$. In fig.14b the relative resistance of a mono-crystal of Bi at 30 and 75°C in 2 directions Φ is given as function of P, the Φ angle between this direction and the long axis of the crystal is 8° (//) and 75° (⊥), the data come from Table XIV of ref. [3]. Plain lines are linear fits, for each direction the 2 isotherms are parallel and the thermal pressures at constant R in the two directions are $(dP/dT)_{R//}$ = -15 $MPaK^{-1}$ and $(dP/dT)_{R//}$ = -25 $MPaK^{-1}$.

Assuming that the thermal pressure $(dP/dT)_R$ of the poly-crystalline sample is (1/3) $(dP/dT)_{R//}$ +(2/3) $(dP/dT)_{R//}$, one concludes that $(dP/dT)_R$= -21 $MPaK^{-1}$ in total agreement with the slope dP/dT_m = - 20 $MPaK^{-1}$ of the melting curve of Bi (rhombohedric structure) near Tm(P=10 kbar) ~ 500 K.

Strontium shows the same behavior, see figure 70 of ref. [3], the three isotherms curves R(P) at 0 50 and 100°C can be superposed by the constant translation ΔP . The thermal pressure is $(\Delta P/\Delta T)_R$ = - 5.6 $MPaK^{-1}$, from Table XIV of this reference one deduces a similar value - 5 $MPaK^{-1}$. Between 0 and 100 °C Sr presents a crystalline phase transition (fcc → bcc) at Ttr, the slope dP/dTtr is negative, about - 3 to – 4 $MPaK^{-1}$. In conclusion Strontium and Bismuth verify the Slatter and the V ~ R conjectures, rel. 4e with k_{Ir}=1, $dP/dTtr = (dP/dT)_R$.

The thermal pressure at constant resistivity of various elements in liquid and crystalline phases (poly-crystal and mono-crystal) are compared in Table 5; "normal" conductors (K Na Hg Pb) and "abnormal" conductors (Bi Sr black P). The thermal pressure data $(dP/dT)_R$ comes from the Bridgman works at low temperature, 0<T<200°C. In the last column are given the slopes of the phase transition curves, Tm(P) T_{tr}(P), which occurs at low pressure in the T-P domain of the resistivity measurements; for metals and alkali see Table 2 and Table 3 of ref. [17], for Bi Sr P see the phase diagrams in ref. [65-67].

From this Table ones concludes that:

a) The thermal pressures at constant V and R are of the same order whatever is the state of the element, liquid or solid in different crystalline states, whatever is the direction of measurement in a single crystal.

b) Just above the T and P domains of measurement of the thermal pressures the elements (normal and abnormal) presents a first order phase transition (melting or crystalline transition) the slopes dP/dTm and dP/dTtr of the transition curves and the thermal pressure $(dP/dT)_R$ at constant R have same sign and are of the same order.

	State	$(dP/dT)_R$ MPa/K	$(dP/dT)_V$ MPa/K	dP/dTm or dP/dTtr MPa/K
K	p - cr	2 – 2.8	(0.6)	7.5 - 8.6 sol-liq
Na	p - cr liq	4.5 7	(1.4)	11 sol-liq
Hg	m-cr - α m-cr - β liq	 2.6	(4.4) (5.3) (3.8)	4.5 β → α
Pb	p-cr	22		13 sol-liq
Bi	p - cr m-cr // m-cr ⊥	- 16 - 13 - 22		- 19 Rh →liq
Sr	p- cr	-5 – 5.6		-7 fcc→ bcc
P	p - cr	-3.2		-6 -10 orth→rhom

Table 5: Thermal pressures $(dP/dT)_R$ and $(dP/dT)_V$ at constant resistivity and volume of various elements determined at low temperature, 0<T<100°C, data from the works of Bridgman, ( ) values are from ref. [17]

dP/dT_m and dP/dT_{tr} are the slope of the transition curves P(Tm) (melting) and $P(T_{tr})$ (crystalline transition) appearing just above 100 °C, data from ref. [65], see text. p-cr: poly-crystalline, m-cr: mono-crystalline

Conclusion

We have analyzed the correlation between the resistivity and specific volume of most conductor "normal" and "abnormal" materials in the polycrystalline and monocrystalline states in the amorphous and liquid states. In the solid and liquid states all the materials follow at constant T the same equation of state m-VW EOS ($V \sim R \sim 1/(P+P^*)$ and at constant pressure P the same power law $V \sim R \sim T^n$ (rel. 2, solid n ~ 1.27; liquid n = 1). In glassy metals below the glass transition the dependence of R and V with the aging time follow the same logarithmic law (rel.6). The observed properties deduced from this EOS and the power laws (rel. 2 and 6) are the following:

The characteristic pressure P*

From the fit of the V(T,P) and R(T,P) data with the m-VW EOS the same characteristic pressure P* is deduced. The relation P*(V) = P*(R) (figure 2e, Table 2a and Table 4) is valid whatever is the state of the material (melt glass or crystal).

The FST-Is

The tangents to the isotherms V(P) and R(P) of metallic elements at low pressure in the solid and liquid states converge at the same characteristic pressure P* deduced from the m-VW EOS fit. The P* values deduced from the FST-Is of poly-crystalline and mono-crystalline metallic samples are also in excellent agreement with this EOS P* value.

The characteristic relative resistivity r* and volume v*

The relative resistivity $r^*=R^*/R_0$ and volume $v^*=V^*/V_0$ deduced from m-VW EOS are compared in Table 2b. The volume V* and the resistivity R* extrapolated at 0 K are deduced from the power laws above and below Tm. By extrapolation of the data above the residual resistivity domain $T > T0^* \sim 40$ K and Tm one finds that r* is negligible ($r^* \sim v^*/10$) and that the ratios of the thermal components v = V-V* and r = R-R* of the solid and liquid states of transition metals are of the same order at any temperature, vL / vs ~ rL / rs ~ 2 (Table 1b).

The superposition principle

The isotherm curves V(P) and R(P) of all the metallic elements ("normal" and "abnormal") verify this principle. The thermal pressures $(dP/dT)_V$ and $(dP/dT)_R$ (Tables 3 and Table 5) are of the same order and P and T independent whatever is the state of the element, liquid or solid. In single crystal of Bi it has been shown that these thermal pressures are independent on the direction of measurement and of the order of that of the bulk sample.

The Slater and Bridgman conjectures

Elements which present a melting or a crystalline transition near the domain of resistivity measurements verify relations 4e-4f between the thermal pressures $(dP/dT)_R$ and the slope dP/dTtr or dP/dTm of the transition curve. From Table 5 one concludes that the Slater parameter, $k_{tr} = (dP/dT)_R / (dP/dTtr)$, of elements with a positive slope (K, Na, Hg) and with a negative slope (Bi, Sr, P) is of the order $k_{tr} = 1$ to 3 as predicted by the Slater and Bridgman conjectures, rel.4e,f.

The volume and resistivity jumps at the melting transition

The jumps ΔVtr and ΔRtr at the melting and crystalline transitions are linear functions of the pressure ($P<P^*$) and extrapolate to zero at P*. Rel. 5 deduced from the m-VW EOS is verified.

Open Questions

This comparison between volume and resistivity properties based on the m-VW EOS and the scaling laws leads to new questions:

a) The isobars R(T) and V(T) are linear functions of T, the FST-Ib is observed at high and low temperature above T^*_0. No change of behavior is observed at the Debye temperature. The resistivity of transition metals in the normal (non superconducting) state extrapolates to zero near the characteristic temperature T* (20 to 75 K), well above the supra-conductivity temperature Tc . Linear relation R(T) and same orders of temperature T* are also observed in metals of the platinum group (Pd, Ir, Rh, Os, Ru) [1]. Liquid Hg, and black phosphorus have completely different (extrapolated) temperatures T* ; -150 K (Hg), and +420 K (b-P). What is the real physical meaning of this characteristic temperature?

b) The ratio α(R) / α(V) of the temperature coefficients of R and V (Table 1) increases with P* thus with the bulk modulus, see ref. *[17]*. The relation α(R) / α(V) = k P* is observed, the constants k is 8.6 GPa^{-1} (alkali) and 2.5 GPa^{-1} (transition metals). What is the influence of the electronic configuration of the elements on this parameter?

c) At low temperature, $T < T^*_0$ (see fg.1c), the resistivity at low pressure (residual resistivity) can be fitted with a power law $R \sim T^n$ but it is well known that at low temperature the experimental data are dependent on the impurity (content and nature) and on the thermal history of the sample (temperature of cycling and annealing, aging time…). To verify the R ~ V conjecture at low

temperature it is necessary to measure the T and P variations of the volume and resistivity accurately on the same sample having same thermal history.

d) According to Bridgman and other few authors the resistivity of alkali metals decrease with P at low pressure and then increases with P at high pressure, P >> P*, the R ~ V conjecture is no longer valid above P*. According to the very rare experiments the minimum of the R(P) curve occurs at Pmin (2 GPa for Na and K) above or near P*, but how to predict this minimum (Rmin, Pmin) as function of the nature of the material ? Is this minimum weakly dependent on T as suggested by Bridgman?

e) As noted by Kraut et al [27], the melting temperature T_m of simple elements and minerals tends to level of at high pressure and in some materials the melting curves $T_m(P)$ present a maximum (examples Na, K, Cs, Ba, ref.[7]). The pressure at the maximum of Tm in Na and K is of the order of the characteristic pressure P*, is it a general empirical rule?

f) The experiments of Bridgman show that in single crystals the resistivity ρ increases linearly with the distances d_x between the reticular planes perpendicular to the electric field. Is ρ along the a and c axis of a metal with a hexagonal structure have the same extrapolated value in different experimental conditions, if the distances d_a (T_1,P_1) and d_c (T_2,P_2) are equal?

g) In any material submitted to a uni-axial or bi-axial pressure (drawing or compressive) the deformation $\lambda(P)=dL/L_0$ is a complex function of P T and time (or deformation rate). Can the static and dynamic processes of deformation of metallic materials be studied by resistivity measurements? By measuring the resistivity parallel and perpendicular to the drawing direction is it possible predict the yield stress the rupture stress and the Poisson coefficient, if the L ~ R conjecture is observed?

Conclusively this review pays tribute to P. W. Bridgman who found out, one century ago, the similarity between the T and P variations of volume and resistivity in a great number of materials. His first researches and then those of many authors afterward verify the prediction of the m-VW EOS and lead to new important questions of fundamental and applied interest.

Reference

1. PW Bridgman (1921) Proceedings Am Acad Arts and Sci 56: 61.

2. PW Bridgman (1948) Proceedings Am Acad Arts and Sci 76: 71.

3. PW Bridgman (1958) The physics of high pressure, Edit. Bell and Sons, London.

4. JP Poirier (1991) Introduction to the Physics of the Earth's Interior, Cambridge University Press.

5. FD Stacey (2005) High pressure equations of state and planetary interiors. Rep Prog Phys 68: 341.

6. JS Dugdal, D Gugan (1962) The effect of pressure on the electrical resistance of lithium, sodium and potassium at low temperatures. Proc Roy Soc A270: 186.

7. A Lacam, M Lallemand (1964) Pressure and composition dependence of the electrical conductivity of iron-rich synthetic olivines to 200 kbar. J Physique 25: 402.

8. GT Meaden (1965) Electrical Resistance of Metals, Plenum Press, New York.

9. LA Hall (1968) Survey of Electrical Resistivity Measurements on 16 Pure Metals in the Temperature Range 0 to 273K. NBS Tech 365: 1–111.

10. RA Matula (1979) Electrical resistivity of copper, gold, palladium, and silver. J Phys Chem Ref Data 8: 1147.

11. NF Mott, H Jones (1936) Theory of the properties of metals and alloys, Oxford.

12. C Kittel (2004) Introduction to Physics of Solid state, John Wiley, New York.

13. JM Ziman (1960) Electrons and phonons, Oxford.

14. Rault (2014) A universal modified van der Waals equation of state. Part I: Polymer and mineral glass formers. Eur Phys J E 37: 113.

15. J Rault (2015) Polymer Glass Formation: Role of Activation Free Energy, Configurational Entropy, and Collective Motion. Eur Phys J E 38: 91.

16. J Rault (2017) The equation of state of polymers. Part III: Relation with the compensation law. Eur Phys J E 40: 82.

17. J Rault (2019) 1-Carbazolyl Spirobifluorene: Synthesis, Structural, Electrochemical, and Photophysical Properties. Eur Phys J B 92: 31.

18. J Rault (2003) Melting of ice in porous glass: why water and solvents confined in small pores do not crystallize? J Phys Condens Matter 15: 1.

19. G Kaptay (2015) Approximated equations for molar volumes of pure solid fcc metals and their liquids from zero Kelvin to above their melting points at standard pressure. J Mater Sci 50: 687.

20. JW Arblaster (2015) Selected Electrical Resistivity Values for the Platinum Group of Metals Part I: Palladium and Platinum. Johnson Matthey Technol Rev 59.

21. JC Slater (1939) Introduction to Chemical Physics, McGraw-Hill N.Y.

22. JP Romain, A Migault, J Jacquesson (1976) Relation between the Grüneisen ratio and the pressure dependence of Poisson's ratio for metals. J Phys Chem Solids 37: 1159-1165.

23. L Gerward (1985) The bulk modulus and its pressure derivative for 18 metals. J Phys Chem Solids 46: 925-7.

24. P Vinet, JH Rose, J Ferrante, JR Smith (1989) Universal features of the equation of state of solids. J Phys Condens Matter 1: 1941.

25. IC Sanchez, J Cho, WJ Chen (1993) Universal response of polymers, solvents, and solutions to pressure. Macromolecules 26: 4234-41.

26. ER Grilly, RL Mills (1957) Volume Change on Melting of N 2 up to 3500 kg/ cm^2. Phys Rev 105: 1140.

27. CA Swenson (1958) Phase Transition in Solid Mercury. Phys Rev 111: 82.

28. RW Keyes (1958) Volumes of Activation for Diffusion in Solids. J Chem Phys 29: 467.

29. Y Adda, J Philibert (1966) Atom movements - diffusion and mass transport in solids. Diffusion in Solids, PUF, Paris.

30. J Rault (2009) Physical Aging of Glasses: the VFT approach, Nova Science Publishers, N.Y.

31. J Rault (2006) Aging of oriented polymer glasses. J Non-Cryst Solids 352: 4946-55.

32. IN Makarenko, AM Nikolaenko, VA Ivanov, SM Stishov (1975) Equation of state of alkali metals: Sodium. Sov Phys –JETP 42: 875.

33. MS Anderson, CA Swenson (1985) Experimental equations of state for cesium and lithium metals to 20 kbar and the high-pressure behavior of the alkali metals. Phys Rev B 31: 668.

34. A Jayaraman, RC Newton, JM McDonough (1967) Phase Relations, Resistivity, and Electronic Structure of Cesium at High Pressures. Phys Rev 159: 527.

35. S Ayrinhac, M Gauthier, LE Bove, M Morand, G Le Marchand, et al. (2014) Equation of state of liquid mercury to 520 K and 7 GPa from acoustic velocity measurements. J Chem Phys 140: 244201.

36. P Kuchhal, R Kumar, N Dass (1997) Equation of state of liquid metals from sound-velocity measurements. Phys. Rev. B, 55:8042.

37. A Eiling, JS Schilling (1981) Pressure and temperature dependence of electrical resistivity of Pb and Sn from 1-300K and 0-10 GPa-use as continuous resistive pressure monitor accurate over wide temperature range; superconductivity under pressure in Pb, Sn and In. J Phys F Metal Phys 11: 623.

38. BN Aleksandrov, IG D'Yakov (1963) Survey of Electrical Resistivity Measurements on 8 Additional Pure Metals in the Temperature Range 0to273K. Soviet Phys JETP 16: 603-08.

39. JP Romain, A Migault, J Jacquesson (1976) Relation between the Grüneisen ratio and the pressure dependence of Poisson's ratio for metals. J Phys Chem Solids 37: 1159-65.

40. K Shimizu, T Kimura, S Furomoto, K Takeda, K Kontani, et al. (2001) Superconductivity in the non-magnetic state of iron under pressure. Nature 412: 316.

41. SE Babe (1962) J Chem Phys 37: 922.

42. E Knittle (1995) Static compression measurements of equations of state. Mineral Physics and Crystallography: A Handbook of Physical Constants 2: 98-142.

43. Fang-Qiu Zu , Rong-Rong Shen, Y Xi, Xian-Fen Li, Guo-Hua Ding, et al. (2006) J Phys Condens Matter 18: 2817.

44. VG Bar'yakhtar, LE Mikhailova, AG Il'inskii, AV Romanova, TM Khristenko (1989) Sov Phys JETP 68: 811.

45. DR Lide (2009) CRC Handbook of Chemistry and Physics, Boca Raton, CRC Press Inc.

46. See references in https://enwikipedia.org/Tin.

47. M Berrada, RA Secco, W Yong (2018) Decreasing electrical resistivity of gold along the melting boundary up to 5 GPa. High Pressure Res 38: 367-76.

48. NQ Hoc, BD Tinh, ND Hien (2020) Efficient Analytical Approach for High-Pressure Melting Properties of Iron. Mat Res Bulletin 128: 110874.

49. SH Shim, TS Duffy, T Kakenichi (2002) Equation of state of gold and its application to the phase boundaries near 660 km depth in Earth's mantle. Earth Plan Sci Letters 203: 729.

50. SM Clark, JM Zaug (2010) Compressibility of cubic white, orthorhombic black, rhombohedral black, and simple cubic black phosphorus. Physical Review B 82: 134111.

51. G Monaco, S Falconi, WA Crichton, M Mezouar (2003) Nature of the First-Order Phase Transition in Fluid Phosphorus at High Temperature and Pressure. Phys Rev Lett 90: 255701.

52. CY Ho, TK Chu (1977) Thermal Conductivity and Electrical Resistivity of Eight Selected AISI Stainless Steels. Cindas report 45.

53. PD Desai, CY Ho (1978) Thermal Linear Expansion of Nine Selected AISI Stainless Steels. Cindas report 51.

54. P Allia, R Sato Turtelli, F Vinai, G Riontino (1982) Free volume dependence of the electrical resistivity of metallic glasses prepared with different quenching rates. Solid State Communication 43: 821-4.

55. KF Kelton, F Spaepen (1984) Kinetics of structural relaxation in several metallic glasses observed by changes in electrical resistivity. Phys Rev B 30: 5516.

56. M Valanathan (1998) Thesis, Durban. http://hdl.handle.net/20.500.11892/76878

57. P Limelette, P Wzietek, Florens, A Georges, TA Costi, et al. (2003) Phys Rev Letters 91: 016401.

58. H Hegger, C Petrovic, EG Moshopoulou, MF Hundley, JL Sarrao, et al. (2000) Pressure-Induced Superconductivity in Quasi-2D CeRhIn 5. Phys. Rev. Letters, 84: 22.

59. JK Bao, JY Liu, CV Ma, ZH Meng, ZT Tang, et al. (2015) Superconductivity in Quasi-One-Dimensional $K_2Cr_3As_3$ with Significant Electron Correlations. Phys Rev X 5: 011013.

60. N Doiron-Leyraud, P Auban-Senzier, SR de Cotret, C Bourbonnais, D Jerome, et al. (2009) Correlation between linear resistivity and Tc in the Bechgaard salts and the pnictide superconductor Ba(Fe1−xCox)2As2. Phys Rev B 80: 214531.

61. A Legros, S Benhabib, W Tabis, F Laliberte, M Dion et al. (2019) Proust, Nature Physics, Nature Publishing Group 142-7.

62. MS Anderson, CA Swenson (1974) Experimental compressions for normal hydrogen and normal deuterium to 25 kbar at 4.2 K. Phys Rev B 10: 5184.

63. S Jiuxun, W Qiang, C Lingcang, J Fukqian (2006) The modified van der Waals equation of state. Physica B 371: 257.

64. ST Weir, AC Mitchell, WJ Nellis (1996) Metallization of Fluid Molecular Hydrogen at 140 GPa (1.4 Mbar). Phys Rew Letters 76: 1860.

65. DA Young (1991) Phase Diagrams of the Elements University of California Press.

66. RW Powell, RP Tye, MJ Woodman (1962) Thermal Conductivities and Electrical Resistivities of the Platinum Metals. Platinum Metals Rev 6: 138.

67. EA Kraut, GC Kennedy (1966) New Melting Law at High Pressures. Physical Review Phys Rev 151: 668.